Project-level instantaneous emission modeling from mobile sources for freeway lane closure using SHRP2 Naturalistic Driving Study data and microscopic traffic simulation

by

Georges Bou-Saab

A dissertation submitted to the graduate faculty

in partial fulfillment of the requirements for the degree of

DOCTOR OF PHILOSOPHY

Major: Civil Engineering (Transportation and Environmental Engineering)

Program of Study Committee:
Shauna Hallmark, Co-major Professor
Omar Smadi, Co-major Professor
Basak Aldemir Bektas
James Alleman
Jing Dong
Jacek Koziel

The student author, whose presentation of the scholarship herein was approved by the program of study committee, is solely responsible for the content of this dissertation. The Graduate College will ensure this dissertation is globally accessible and will not permit alterations after a degree is conferred.

Iowa State University

Ames, Iowa

2019

DEDICATION

"I wouldn't be where I am today without the constant support from my family and close friends."

الى كل يلي بحبوني

TABLE OF CONTENTS

LIST OF FIGURES

LIST OF TABLES

ABSTRACT

This dissertation is one of the first studies which used the Second Strategic Highway Research Program (SHRP2) Naturalistic Driving Study (NDS) data to perform modal emission modeling at the project-level. SHRP2 NDS was the largest naturalistic driving study to date conducted in the U.S. which included instrumented vehicles with over 3,000 drivers that were recruited from six states. There is great potential to apply this data in modeling emissions as it will capture differences in driver behavior, roadway geometry, traffic conditions and their impact on emissions. The dissertation had two primary objectives: (1) apply the SHRP2 NDS data to model instantaneous exhaust emissions from passenger vehicles at four-lane divided freeway segments with work zones, and (2) examine the accuracy of microscopic traffic simulation models to replicate real-world vehicle trajectories in order to estimate emissions at work zones.

Research studies related to assessing the impact of lane closure on vehicular emissions are limited considering that collecting data from field observations is resource intensive and expensive. In addition, the application of microsimulation models instigates certain constraints because various driver behavior and lane changing parameters must calibrated to ensure that the output from traffic simulation models can represent accurate real-world driving activity. Therefore, the first study focused on utilizing the vehicle kinematics data collected as part of the SHRP2 NDS to model emissions from passenger cars for work zones employed on four-lane divided principal arterials. The emissions models in this study considered different work zone configurations and varying congestion levels. Furthermore, the second analysis examined the ability of Vissim microsimulation model to replicate field conditions. A generic guidance to calibrate the

driver behavior parameters in Vissim for freeway lane closure was applied and findings were compared to field observations from the SHRP2 study. Three different construction scenarios were implemented, i.e. AM-peak hour, PM-peak hour and nighttime off-peak lane closure.

CHAPTER 1. GENERAL INTRODUCTION

During the past four decades, there has been discrepancies between the number of vehicle-miles traveled (VMT) and total roadway mileage in the United States (U.S.). VMT increased drastically, by approximately 110 percent, between 1978 and 2018 (*1*), whereas the total lane-miles of all functional classes increased by only 10 percent (*2*). In 2018, each driver in the U.S. lost more than 90 hours on the roads due to congestion resulting in a total cost of $87 billion, an average of $1,348 per driver (*3*). Consequently, Congress passed a bill in 2015, Fixing America's Surface Transportation Act (FAST Act), to help regulate the federal investment on surface transportation. The bill was signed by the U.S. administration to fund surface transportation programs with the aim to increase mobility on highways, support economic growth, accelerate project delivery and promote innovation. FAST Act builds on the changes made by the Moving Ahead for Progress in the 21st Century Act (MAP-21) which was enacted in 2012 (*4*). One of the important provisions of MAP-21 is to reduce traffic congestion and improve efficiency of the roadway system. Consequently, the number of road construction projects has increased to address the challenges facing the U.S. transportation system. Most active work zones are installed on major urban roadway networks that are already congested hence, negatively impacting mobility and safety of drivers. A significant portion, nearly 24 percent, of the non-recurring delay on freeways was accounted by work zones in 2014 (*5*). Road closure due to reconstruction and rehabilitation projects resulted in 10 percent of overall congestion with an estimated annual fuel loss of 310 million gallons.

Aggravated traffic congestion is partly attributed to the increase in vehicle ownership while delay is primarily caused by non-recurring incidents such as crashes and

roadway construction (*6*). With heightened safety issues and the fact that drivers have to spend more time on the roads, non-recurring events can adversely impact air quality. For example, pavement construction and rehabilitation contributes to a substantial share of vehicle emissions (*7*) and lower fuel economy. Emissions are also altered with the transportation of materials to the sites and the operation of heavy equipment. The transportation sector is a major contributor to air pollution in the U.S. with on-road mobile sources accounting for almost 35 percent of total carbon dioxide (CO_2) in the atmosphere (*8*). Nitrogen oxides (NO_x), particulate matter (PM) and volatile organic compounds (VOCs) are other harmful pollutants from surface transportation which are known to trigger serious health and environmental effects both locally and regionally (*9 and 10*). Regardless of the substantiated implementation of national programs and standards for fuels and vehicles to reduce smog and soot from transportation sources (*9*), factors such as steady growth in VMT and aging infrastructure guarantee that the pollutant component of emissions will remain a priority (*11*).

Objectives

There are limited studies quantifying the impact of work zones on emissions due to the lack of field observations. State-of-the-practice emissions rate models require disaggregate vehicle activity data as inputs. Previous efforts relied on instrumented vehicles or chase car technique to collect field data. However, these methods are resource intensive and expensive (making it difficult for local transportation agencies to afford). Other efforts used micro-simulation to obtain data but various driver behavior and lane changing parameters must calibrated. This is required in order to validate that the output from traffic simulation models can represent accurate real-world driving activity.

Research Objectives:

(1) Estimate emissions of criteria pollutants and greenhouse gases for work zones on 4-lane divided principal arterials with different configurations.

(2) Investigate the capability of traffic microsimulation tools to replicate field conditions to accurately estimate vehicle emissions at work zones.

Approach:

- Objective (1): utilize the second strategic research highway program naturalistic driving study data (SHRP2 NDS). The analysis will also consider work zone principal areas and level of congestion.

- Objective (2): Vissim will be used to simulate different lane closure scenarios in a case study and results will be compared to the SHRP2 NDS findings.

Rationale:

- Objective (1): Many researchers showed interest in the SHRP2 NDS data to conduct safety and driver distraction studies. One major benefit of using such a dataset is that it represents the overall vehicle fleet, driver population and traffic conditions in the U.S. There is potential to utilize this data in modal emission modeling at project-level by acquiring second-by-second speed and acceleration to calculate vehicle specific power then assign data to different operating mode bins to estimate emissions. Overall, results from this research will help agencies understand how driver behavior impacts emission from passenger cars for varying scenarios and decide on the appropriate work zone configuration given traffic and roadway information.

- Objective (2): Taking into consideration that various local agencies cannot collect field data, traffic simulators can be used to model the traffic flow in a network. Traffic microsimulation can improve the precision of quantifying environmental impacts in transportation cost-benefit analysis. Different lane closure scenarios will be implemented, and results will be compared to the SHRP2 NDS findings.

Organization of the Dissertation

The contents of the dissertation are divided into four chapters:

(1) Chapter 1 provides an overview of the research project and addresses the problem statement. The objectives are also identified in this chapter.

(2) Chapter 2 examines the use of SHRP2 NDS data to model instantaneous vehicular emissions at work zones. The study framework presented in Chapter 2 will focus on analyzing emissions from passenger cars traversing along work zones employed on four-lane divided freeway segments.

(3) Chapter 3 investigates the feasibility of Vissim, a traffic microsimulation model, to generate real-world vehicle trajectories. It is well-established in the literature that second-by-second vehicle kinematics are important inputs in current emissions models. One particular work zone location from the SHRP2 NDS in the second chapter is used as a case study and characteristics of the work zone in terms of configuration and length of different components are verified. Different construction scenarios will be tested and results from the microscopic model will be compared to the SHRP2 findings using multiple metrics.

(4) Chapter 4, the final chapter, includes a general summary of the tasks performed in

this dissertation and provides recommendations for future research work.

References

1. Policy and Governmental Affairs. *Traffic Volume Trends*. Office of Highway and Policy Information, FHWA. https://www.fhwa.dot.gov/policyinformation/travel_monitoring/tvt.cfm. Accessed February 2, 2019.

2. *National Transportation Statistics 2018*. Bureau of Transportation Statistics, U.S. DOT. https://www.bts.gov/product-type/national-transportation-statistics. Accessed February 2, 2019.

3. INRIX: Congestion Costs Each American 97 Hours, $1,348 a Year. Press Releases, INRIX. http://inrix.com/press-releases/scorecard-2018-us/. Accessed January 28, 2019.

4. *Fixing America's Surface Transportation Act (FAST Act)*. FHWA, U.S. Department of Transportation. https://www.fhwa.dot.gov/fastact/. Accessed February 2, 2019.

5. Work Zone Management Program. *Facts and Statistics – Work Zone Safety*. Office of Operations, FHWA. https://ops.fhwa.dot.gov/wz/resources/facts_stats/safety.htm. Accessed February 5, 2019.

6. Avetisyan, H. G., E. Miller-Hooks, S. Melanta and B. Qi. Effects of Vehicle Technologies, Traffic Volume Changes, Incidents and Work Zones on Greenhouse Gas Emissions Production. *Transportation Research Part D: Transport and Environment*, 2014. 26: 10 – 19.

7. Zhang, K. S. Batterman and F. Dion. Vehicle Emissions in Congestion: Comparison of Work Zone, Rush Hour and Free-flow Conditions. *Atmospheric Environment*, 2011. 45: 1929 – 1939.

8. *California Greenhouse Gas Emission Inventory, Scoping Plan Categorization*. California Air Resources Board (CARB). https://www.arb.ca.gov/cc/inventory/data/data.htm. Accessed February 5, 2019.

9. Transportation, Air Pollution and Climate Change. *Smog, Soot, and Other Air Pollution from Transportation*. U.S. Environmental Protection Agency. https://www.epa.gov/transportation-air-pollution-and-climate-change/smog-soot-and-local-air-pollution. Accessed February 9, 2019.

10. Litman, T. Evaluating Carbon Taxes as an Energy Conservation and Emission Reduction Strategy. *Transportation Research Record: Journal of the Transportation Research Board*, 2009. 2139: 125 – 132.

11. *Guidelines for Quantifying Vehicle Emissions within the Ministry's Multiple Account Evaluation Framework*. British Columbia Ministry of Transportation. https://www2.gov.bc.ca/assets/gov/driving-and-transportation/transportation-infrastructure/planning/guidelines/guidelines_emissions.pdf. Accessed January 28 2019.

CHAPTER 2. PROJECT-LEVEL EMISSION MODELING AT WORK ZONES USING SHRP2 NDS DATA

Modified from a manuscript published in: TRB e-Circular E-C243: SHRP 2 Safety Data Student Paper Competition 2017-2019

"Beyond Safety: Utilizing SHRP2 NDS Data to Model Vehicular Emissions from Passenger Cars at Work Zones Using Vehicle Specific Power and Operating Mode Distribution Approach"

Authors: Georges Bou-Saab[1], Shauna Hallmark[1] and Omar Smadi[1]

Affiliation: [1]Iowa State University – Institute for Transportation, Ames, Iowa

Abstract

Transportation sector is a major contributor to air pollution. Therefore, it is essential to monitor vehicular emissions in order to control air quality. Many researchers showed interest in the Second Strategic Highway Research Program (SHRP2) naturalistic driving study (NDS) data to conduct safety and driver distraction studies. One major benefit of using such a dataset is that it represents the overall vehicle fleet, driver population and traffic conditions in the U.S. There is potential to utilize this data in modal emission modeling at project-level by acquiring second-by-second speed and acceleration to calculate vehicle specific power then assign data to different operating mode bins to estimate emissions. The primary focus of this study was to utilize SHRP2 NDS data to estimate emissions of criteria pollutants for work zones in 4-lane divided principal arterials with different configurations. The analysis also considered work zone

principal areas and level of congestion. Overall, results showed that the work zone area type and configuration did not have any impact on emissions. Whereas, high congestion levels increased emissions and predominantly within the activity area. Further investigations by comparing the different bivariate speed and acceleration distributions using the energy statistics showed that work zone configuration and principal area had a significant impact on vehicle operations.

Keywords: Work zones, Second Strategic Highway Program (SHRP2) Naturalistic Driving Study (NDS), Emissions Modeling, Vehicle Specific Power (VSP), Operating mode distribution, MOVES-Matrix, Energy Statistics

Introduction

Work zones are typically employed on roadway networks for restoration, resurfacing, rehabilitation and reconstruction projects. Lane and shoulder closures and other work zone features can reduce capacity and create bottlenecks disrupting traffic flow. Congestion due to work zones on a roadway network is non-recurring since they temporarily interrupt traffic movement. Non-recurring events also include crashes, severe weather conditions, disabled vehicles and special planned events, and they account for approximately 50 percent of total congestion. Work zones are responsible for 10 percent of total congestion (*1*). The impact of work zones is not only limited to mobility, safety and user cost, it also extends to the environment. Congestion occurring at these particular locations contributes to higher tailpipe vehicular emission including carbon dioxide (CO_2), and criteria pollutants: carbon monoxide (CO), gaseous hydrocarbons (HC), nitrogen oxides (NO_x), particulate matter (PM2.5 and PM10). Increase in emissions is

caused by increases in stop-and-go driving and in some cases idling. Besides driving patterns, emissions at work zones are dependent on several significant factors such as facility type, travel demand, detour plans along with spatial and temporal factors (*2*).

Emission Modeling at Work Zones

Research quantifying the impacts of work zone on emissions is limited. Most related available studies examined how varying congestion levels in general impact emissions. A study in Ann Arbor, Michigan estimated emissions under congested and free-flow conditions from light and heavy duty vehicles on a freeway segment (*3*). This was achieved by collecting instantaneous speed and vehicle position from a permanent traffic recorder. The selected freeway segment experienced congestion due to rush hour and presence of a work zone. Zhang et al. used the comprehensive modal emission model (CMEM) to estimate second-by-second emissions. When the traffic transitioned from free-flow to congested condition, CO, HC and NO_x emission rates from light-duty vehicles were the highest. On the contrary, lowest rates were recorded for vehicles moving at low-speed in the congested work zone. As for CO_2 and fuel consumption, the work zone on the freeway under congested traffic flow yielded highest rates. Results for high-duty vehicles differed, as congested work zones contributed to the highest CO, HC and CO_2 emission rates as well as fuel consumption. However, NO_x emissions remained unchanged for different traffic conditions (*3*). Salem et al. (*4*) reviewed various lean construction tools to help them understand how the application of this technique can improve sustainability of work zones. Lean construction techniques lowered vehicle operating cost as mobility and traffic flow conditions improved at work zones, which in return reduced emissions.

Researchers and scientists are constantly assessing new technology and traffic simulation techniques in transportation. For instance, the application of wireless communication technology proved to enhance mobility and safety (*5 and 6*). These systems have the ability to adapt driver behavior to various traffic operations and result in lower emissions. A team of researchers at Texas Southern University examined the impact of introducing a driver smart advisory system (DSAS) in a simulated study where a pedestrian crossing was present in a work zone. The implications of the system changed drivers' behavior as they accelerated smoothly in the work zone and made them stop earlier when faced with a safety-related hazardous situation, i.e. pedestrian crossing the street. Consequently, there was a reduction in vehicle emissions for criteria pollutants (*7*). Another simulated study quantified vehicular emissions at network level for a major freeway corridor reconstruction project in Fort Worth, Texas. The work zone was modeled using a series of links. Capacity and free-flow speed on these links were reduced by dropping the number of lanes. The baseline model consisted of events prior to construction of the work zone. Other modeled scenarios assigned calibrated traffic on the links to compute vehicle emissions as travel behavior changed (*8*). Average emission rate of CO_2, CO, HC and NO_x increased as traffic capacity in the work zone decreased. In a scenario where the capacity was reduced by 50 percent, i.e. 2 lanes dropped, with no diversion of traffic, the average inflow volume and emission rate of criteria pollutants upstream and inside the work zone were comparatively higher than downstream of the work zone (*8*). The simulated study was also implemented on a larger scale regional network in North Carolina which incorporated three major cities, Raleigh, Durham and Chapel Hill. Only passenger cars and passenger trucks were modeled under single and

high occupancy vehicle demand classes. The baseline scenario in the study considered

normal driving conditions with no traffic disturbances. Two other scenarios quantified

congestion and diversion patterns by simulating traffic distribution with the presence of

work zones on a pavement rehabilitation project on I-40 and I-440 corridors in Raleigh.

One of the scenarios considered no diversion (ND) of traffic while the other scenario

diverted traffic to major arterials using user equilibrium (UE) traffic assignment

technique. Results demonstrated that average speed of vehicles and emission levels were

not impacted under the baseline scenario. On the contrary, there was an overall increase

in emissions for ND traffic simulation due to drop in average speed as vehicles started to

queue upstream of the work zones. As noted previously, traffic was diverted to alternate

routes under the UE scenario to reduce congestion upstream and downstream of the work

zone. However, when compared to the baseline scenario, Zhou et al. (*8*) noted that

emission levels were higher in the UE simulation with the formation of a bottleneck at

the work zone.

Effect of Congestion on Emission Levels of Pollutants

Most recently, Texas A&M Transportation Institute (*9*) investigated the air

quality benefits of nighttime construction in urban areas in Texas. Results from three

different case studies suggested that shifting construction activities from daytime to

nighttime reduced total emissions at work zones. This should be expected with lower

traffic volumes at night. However, researchers showed that for similar emission levels,

concentration of pollutants during nighttime might be worsened as a result of changes in

meteorological conditions. With limited number of research pertaining to emission

modeling at work zones, other similar studies involved comprehending the effect of

congestion on emission levels of pollutants. This is considered important while evaluating traffic management strategies. Previous studies analyzed emissions for different roadway types/facilities under varying traffic operation conditions using well-established tools. For instance, freeway air quality was modeled during normal and congested traffic conditions. Salimol Thomas (*10*) developed a framework to model excess emissions during recurring and non-recurring congestion conditions in freeways. A stochastic model was also used to measure the impact of non-recurring incidents on the local emission inventory. Barth and Boriboonsomsin (*11*) utilized CMEM to compute carbon dioxide emissions for different level-of-service (LOS) by categorizing velocity of vehicles as a function of congestion levels. In addition, vehicle emissions on freeways were determined by exploring traffic speeds, freeway capacity and travel demand (*12*). Papson et al. (*13*) used time-in-mode (TIM) methodology to estimate emissions at uncongested and congested signalized intersections under three traffic intersection scenarios. A recent study by Qi et al. (*14*) obtained emission factors for both freeway and arterial facilities under different congestion levels. Findings indicated that emissions were negatively impacted as traffic conditions worsened.

Application of NDS Data in Emission Modeling

Current state-of-the-practice illustrated that capacity was reduced on roadways with construction sites which adversely affected vehicle emissions. Earlier efforts to assess emissions in work zones primarily used average speed and micro-simulated studies to describe vehicle operation which resulted in less reliable results. Exhaust emissions are a function of changes in driver behavior, vehicle kinematics, roadway features and surrounding environment. For increased accuracy in emission modeling at project-level,

second-by-second speed and acceleration data are required to fully describe the different vehicle operations. These limitations can be addressed with the application of the Second Strategic Highway Research Program (SHRP2) naturalistic driving study (NDS) data. There is great potential to apply SHRP2 NDS data in modeling emissions for different work zone configurations at project-level. This will capture differences in driver behavior, roadway geometry, traffic conditions and their impact on emissions. This was the largest naturalistic driving study to date conducted in the U.S. which included instrumented vehicles with over 3,000 drivers that were recruited from six states: Florida (FL), Indiana (IN), New York (NY), North Carolina (NC), Pennsylvania (PA) and Washington (WA). The study consisted of over 5.5 million trip files with almost 40 million miles of data that can be analyzed extensively by researchers (*15*).

Sun et al. (*16*) developed a new approach to develop optimized representative dive schedules from SHRP2 NDS data. The proposed data processing framework is intended to develop driving cycles for light-duty vehicles using 395 road scenarios and 10 roadway properties which can have an influence on the traffic speed pattern. Drive cycles, also referred to as drive schedules, are a series of vehicle speed trajectory points which are essential in modeling since emissions vary with driving patterns (*17*). Other contributing factors include speed limits, traffic conditions, road grade and curvature. Various agencies develop drive cycles to represent the driving conditions unique to a particular geographic area or roadway type. They are also used in the U.S. for federal certification purposes in chassis dynamometer tests to measure tailpipe emissions and fuel economy. In another NDS, Liu et al. (*18*) proposed a plan to generate synthesized drive cycles for pick-up trucks that capture the principles of naturalistic driving. The

drive cycles can be used to optimize the design and control of pick-up trucks taking into account the rigorous federal fuel consumption and emission standards. The University of Michigan quantified and characterized fuel consumption rate of different drivers (*19*). This was accomplished with a well-designed NDS in Michigan where they instrumented 117 identical passenger cars and collected over 210,000 miles of data. Furthermore, North Carolina State University conducted a small-scale NDS and collected high resolution data at 1 Hz frequency using a local sample of 35 drivers. They developed eco-driving metrics by inspecting 20 million seconds of naturalistic driving data to extract the different driving styles and measure their impact along with other confounding factors on fuel consumption (*20*).

Objectives

Emission of criteria pollutants and greenhouse gases from passenger cars can be estimated for work zones at the project-level with the application of a modeling system. In the past, predicting emissions for different transportation elements or networks relied on average speed, whereas recent models account for vehicle operating modes, i.e. instantaneous speed and acceleration, and time spent idling. Accurate estimation of emissions requires second-by-second data since emission rates are highly sensitive to changes in operating modes (*21*). If average speed was used to describe an element or group of elements, then results can be either overestimated or underestimated.

The application of modal modeling allows for second-by-second estimation of emissions and fuel consumption. A robust database of instantaneous speed and acceleration is required and SHRP2 NDS is a prominent source of such data. Roadway and traffic characteristics are linked to the study sites using roadway information

database (RID) which makes it possible to include roadway characteristics. The SHRP2

NDS collected vehicle kinematics at 10 Hz frequency including speed, acceleration,

brake status, gas pedal state and etc. The study also recorded forward view videos and

vehicle position at 1 Hz frequency which can be joined with attributes from RID using

GPS to determine roadway features such as presence of signs and barriers in work zones.

The primary focus of the research effort described in this paper is to model

emissions from passenger cars for different work zone configurations under varying

congestion levels on 4-lane divided principal arterials. SHRP2 NDS data will be applied

in a disaggregate approach at project-level to examine changes in vehicle operations then

acquire emission rates from MOVES-Matrix (*22*) modeling tool. This modeling system is

configured by a team of researchers at Georgia Institute of Technology and is adapted

from the Motor Vehicle Emission Simulator (MOVES) model which is developed by the

United States Environmental Protection Agency (USEPA) to estimate emissions from on-

road vehicles in the United States.

Research Study Methodology

The methodology consisted of the following tasks that were completed to investigate the

impact of various work zone configuration and level of congestion on vehicular

emissions:

Work Zone Identification

Potential work zones during the implementation of the SHRP2 NDS were

identified using 511 data (*23*). A minimum duration of three days was selected for work

zones since the probability of finding sufficient NDS time series data was low for short-

duration projects. Following the identification of 9,290 potential work zones, the location of work zone trips were then determined by linking the 511 events to RID. This also made it possible to estimate the physical extent of the work zones. The number of traces and unique drivers along with demographic characteristics, such as age and gender, of each driver were requested from VTTI. Road construction projects with at least 15 trips were selected which refined the number of potential work zones to 1,680. Another request was then placed for time-series traces 1.5 miles upstream and downstream of the start of a work zone in addition to front and rear-view video logs (*23*). VTTI provided approximately 9,000 traces. However, traces with at least 90 percent of speed data were considered for data reduction. Ultimately, the number of traces was reduced to 5,000. Data points with missing speed information, linear interpolation technique was used to construct new data points within the range of a discrete set of known speed points.

Data Reduction

The roadway functional class for each trace was determined from the RID which facilitated the identification of events used in the data reduction process. A trace is defined as one driver trip through one work zone. Presence of a work zone was confirmed by reviewing the corresponding forward roadway video. Work zone principal area type and configuration along with congestion level were also recorded from forward roadway videos. Some traces did not have a work zone available or were not active. While other traces had traffic signals or non-work-zone related factors that might have interrupted traffic flow (*23*). As a result, they were excluded from analysis. A total of 532 traces were coded. The sampled traces represented three states, NY, PA and WA, and the fleet

consisted of passenger cars. Table 1 provides a description of work zones from every state in terms of unique number of work zones and rural/urban designation.

Table 1. Number of Unique Work Zones by State and Rural/Urban Designation

State	Number of Unique Work Zones	Rural/Urban Designation
New York	13	1: Rural and 12: Urban
Pennsylvania	25	20: Rural and 5: Urban
Washington	7	7: Urban

Work Zone Classification

Work zones were categorized according to their structure along with roadway facility, lane closure configuration, and level-of-service (LOS). For emission analysis, work zones were divided into three principal areas:

- Upstream: Also referred to as the base condition which represents speed traces of vehicles under normal driving condition, i.e. before entering the work zone influence area.

- Advanced warning area: Section of the highway between the first sign observed on the highway system and the start of the work zone which informs drivers about any upcoming roadway construction or incident (*24*).

- Activity area: Typically defined as the section of a highway within the vicinity of any roadway construction (*24*). For analysis purposes, the activity area was identified as the location between the start of the shoulder taper and end of a work zone. In few cases, the trace ended within the work zone.

Emissions from advanced warning and activity area were compared to the baseline condition. Besides area type, the configuration of a work zone which described the layout of the activity portion of a work zone was classified into three categories:

- Shoulder closure only

- Shoulder and lane closure

- Complex configuration (usually starts with shoulder and lane closure then traffic is redirected to opposite direction of travel in a head to head configuration)

Congestion has a significant impact on vehicle operation and tailpipe emissions. Therefore, level of congestion for each trace was subjectively determined from forward roadway videos before a vehicle entered the activity area and by grouping traffic density/LOS into three categories. The categories were defined by Virginia Tech Transportation Institute (VTTI) who collected the SHRP 2 NDS (*25*). The three different classifications for congestion level included the following and it should be noted that this designation of congestion level differs from traditional definitions of LOS:

- Non-congested: LOS A (free-flow condition) or LOS B (stable flow with some restrictions due to presence of other vehicles in traffic stream)

- Moderate congestion: LOS C (stable flow with restrictions in speed and maneuverability due to the presence of leading and adjacent vehicles) or LOS D (high traffic density but stable flow with severe restrictions in speed and maneuverability)

- High congestion: LOS E (unstable flow with traffic operations already at capacity and vehicles are traveling at low speeds with temporary stoppage and inability to maneuver) or LOS F (unstable flow with traffic operations below capacity and vehicles are in stop-and-go condition)

19

Using the categories above, LOS can only be estimated for the conditions surrounding

each subject vehicle. Therefore, it was more appropriately a measure of activity at one

particular location and does not represent LOS for the roadway segment in general.

Figure 2 shows an example of how the three different congestion levels were coded.

Taking into consideration that work zones were initially categorized according to

their area type, a minimum threshold for distance was set for each section: 500 meters

(1/3 of a mile) for upstream section and 800 meters (1/2 of a mile) for both advanced

warning and activity area. Not all traces were used to evaluate each section. In other

words, a trace might not meet the minimum distance requirement for each principal area.

Failure to meet the distance requirement might not essentially capture complete vehicle

operation within a particular work zone component. Moreover, emissions will be factored

in compliance with the distance limits established. The resulting number of traces for

each work zone classification are summarized in Table 2.

Table 2. Number of Traces by Principal Area Type and Congestion Level

Upstream Traces		
	Non-congested	Moderate Congestion	High Congestion
Shoulder Closure	50	144	16
Shoulder and Lane Closure	77	20	8
Complex Configuration	89	29	9
Advanced Warning Area Traces		
	Non-congested	Moderate Congestion	High Congestion
Shoulder Closure	23	37	6
Shoulder and Lane Closure	98	23	9
Complex Configuration	94	34	8
Activity Area Traces		
	Non-congested	Moderate Congestion	High Congestion
Shoulder Closure	29	112	15
Shoulder and Lane Closure	112	23	8
Complex Configuration	106	34	9

Characteristics of each work zone in NY, PA and WA are summarized in Tables 3, 4 and 5, respectively. These primarily include descriptive statistics for the length of the advanced warning area and activity area. The total number of traces that were reduced and the number of unique drivers for each work zone are also included in the tables.

Table 3: Length Characteristics and Traces Information for Work Zones in NY

Work Zone ID	Advanced Warning Area Length (ft.)			Activity Area Length (ft.)			Unique Drivers	Total Traces
	Minimum	Median	Maximum	Minimum	Median	Maximum		
NY1	1886	1919	7123	846	883	7156	11	15
NY2	354	5479	9219	719	4490	6175	15	24
NY3	2346	4972	5367	945	6931	7392	26	36
NY4	1909	6960	8596	856	1988	4675	24	26
NY5	7	10	4436	902	2277	8944	7	15
NY6	5715	9003	9160	617	1699	4839	5	7
NY7	961	4869	5984	1171	6732	8996	26	31
NY8	7	85	2756	525	2257	3757	23	23
NY9	1713	1896	2037	6719	6929	7306	10	19
NY10	1053	2736	5495	607	2300	5574	15	16
NY11	4360	4938	5033	948	6867	7753	16	16
NY12	4977	6170	6276	7920	7923	28169	4	4
NY13	4882	6007	6867	2490	2616	6929	4	4

Table 4: Length Characteristics and Traces Information for Work Zones in PA

Work Zone ID	Advanced Warning Area Length (ft.)			Activity Area Length (ft.)			Unique Drivers	Total Traces
	Minimum	Median	Maximum	Minimum	Median	Maximum		
PA1	1508	3798	5472	3909	10223	11289	21	26
PA2	2578	5655	5868	9969	10144	10434	11	21
PA3	2511	2591	2634	8611	9732	10055	11	12
PA4	2650	5137	5318	9038	9193	9643	10	11
PA5	2587	2593	2600	11356	11381	11406	2	2
PA6	4996	4996	4996	4373	4373	4373	1	1
PA7	2425	5351	10170	8063	12288	14997	6	6
PA8	5038	5091	5550	7279	7400	7577	6	6
PA9	1019	1031	1139	1980	2075	2124	2	3
PA10	4967	5453	8444	1931	4720	5337	9	16
PA11	2326	4727	4767	4999	7729	7788	2	8
PA12	2583	5149	5445	17234	17980	19463	8	11
PA13	10882	10953	11120	5322	5333	5474	3	3
PA14	2424	5526	5667	1653	2233	2667	3	5
PA15	2524	2563	2639	5287	5366	5477	11	11
PA16	9743	9743	9743	3387	3387	3387	1	1
PA17	923	954	2345	4929	7617	7639	1	10
PA18	5289	5436	5511	9248	9709	9836	5	7
PA19	5489	5531	5572	3257	4644	6031	2	2
PA20	5046	10394	16887	2112	4502	5713	6	7
PA21	5499	7840	10180	7921	7930	7938	2	2
PA22	10527	10815	11258	4711	5098	5488	4	4
PA23	9454	15439	21403	3007	3291	3456	5	8
PA24	9564	9789	10013	2744	2752	2761	2	2
PA25	1486	5250	10693	4981	7624	10402	3	7

Table 5: Length Characteristics and Traces Information for Work Zones in WA

Work Zone ID	Advanced Warning Area Length (ft.)			Activity Area Length (ft.)			Unique Drivers	Total Traces
	Minimum	Median	Maximum	Minimum	Median	Maximum		
WA1	4	8	304	8766	9724	12182	9	12
WA2	778	931	3311	9148	11405	11670	8	12
WA3	315	987	1269	8637	10189	10844	13	22
WA4	662	958	1237	9140	11381	13190	18	50
WA5	233	273	312	10052	11164	12275	2	2
WA6	58	58	58	12509	12509	12509	1	1
WA7	6	8	831	8605	10879	11395	5	5

Some work zones had inadequate lengths for the advanced warning area and activity area which were below the minimum distance threshold. As a result, this provides another reason why some traces were excluded from evaluating certain sections of a work zone. As mentioned previously, not all requested traces captured the entire trip of a driver along a work zone. In few cases, the forward roadway video started after the driver entered the vicinity of the work zone and ended within the activity area. In addition, as evident from Tables 3 through 5, some drivers had multiple trips since the number of unique drivers is less than the total number of traces.

Figure 1 illustrates a typical layout of a work zone while Figure 2 shows still images from forward videos as an example of the different congestion levels.
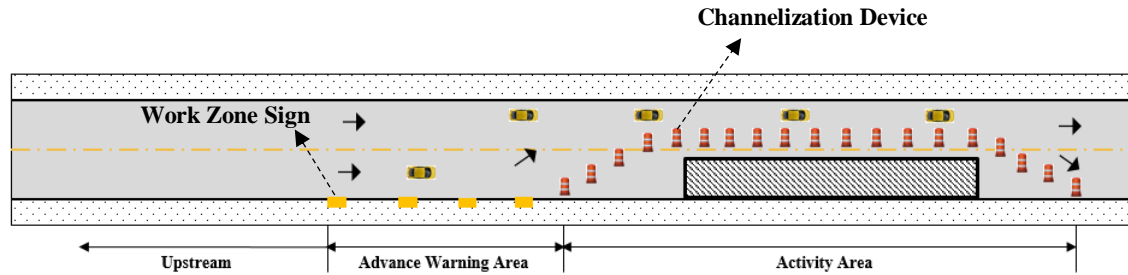
Figure 1. Work zone layout defining the three principal areas (adapted from MUTCD).
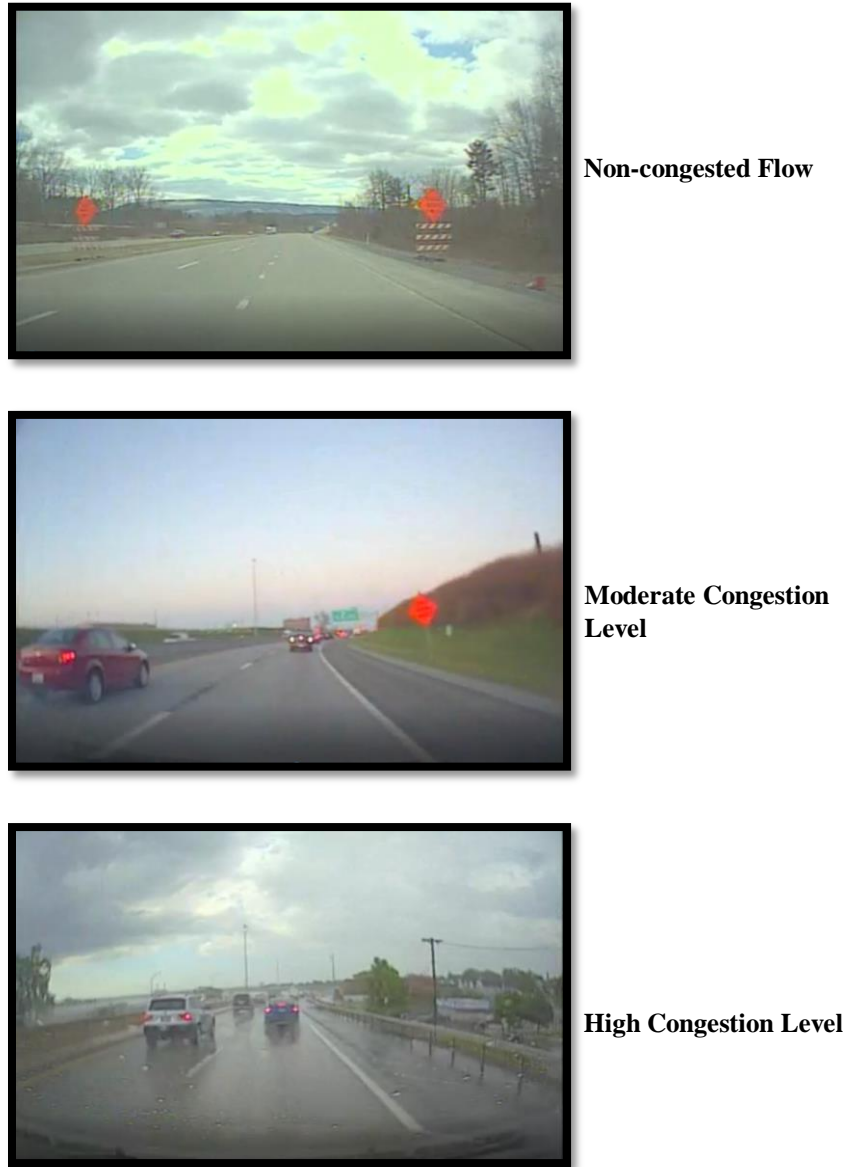
Figure 2. SHRP2 NDS still images showing an example of different level of congestion (Source: VTTI).

Vehicle Specific Power Computations and Operating Mode Distributions

Average speed, driving schedule and operating mode distribution are the three

conventional techniques used to describe vehicle activity in MOVES (*16*) and it is critical

to select an appropriate statistical assessment approach that represents the entire trip.

Operating mode distribution accounts for the fraction of time by operating mode which

includes different bins defined by vehicle specific power (VSP) and vehicle activity (speed ranges, idling, braking and acceleration). This method is more accurate compared to the other two as it effectively enables users to exploit the capabilities of MOVES in modeling emissions as a function of vehicle activity (captures all driving behavior). There is a direct correlation between vehicle emissions and instantaneous engine load demand. The engine load is dependent on speed, acceleration, road grade and air conditioning use. VSP has been used as a proxy variable for power demand or engine load (*26*).

The 10 Hz vehicle activity inputs were converted to 1 Hz by averaging speed every 10 consecutive points to determine speed at one second interval. This will ensure that there is consistency in modeling methodology as the one applied in MOVES which uses second-by-second data. Instantaneous acceleration was then computed by finding the derivative of speed (difference between the current and previous speed points). The second-by-second vehicle activity data were the inputs for the VSP equation (*27*):

$$VSP = \left(\frac{A}{M}\right)v + \left(\frac{B}{M}\right)v^2 + \left(\frac{C}{M}\right)v^3 + (a + g\sin\theta)v \qquad (1)$$

Where,

      A is the road load coefficient for rolling resistance (kW-s/m) = 0.1564

      B is the road load coefficient for rotating resistance (kW-s^2/m^2) = 0.0020

      C is the road coefficient for drag resistance (kW-s^3/m^3) = 0.00049

      M is the fixed mass facto for vehicle source type (metric tons) = 1.4788

      g is acceleration due to gravity (m/s^2)

      v is vehicle speed (m/s)

      a is vehicle acceleration (m/s^2)

      sin θ is fractional road grade

The coefficients for *A*, *B*, *C* and *M* are obtained either specifically for each vehicle type from the manufacturer or from MOVES 2014 highway vehicle population and activity data guide. Only passenger cars were assumed in the analysis. In addition, road gradient was assumed to be flat (i.e. $\theta = 0$) although the information can be linked from RID. These assumptions will ensure better comparisons in emissions by eliminating differences between vehicle types and roadway terrain.

Assignment of Emission Rates to Each Second of Data

Operating mode bins summarized in the MOVES report (*27*) were generated and emission rates were correlated to vehicle activity using a reference table acquired from MOVES-Matrix for the criteria pollutants and greenhouse gases of interest. Total running exhaust emissions were calculated by summing the product of driving activities and corresponding emission rates.

The new adapted tool performs similar emissions modeling and yields exact results as the original MOVES interface but at a faster pace. The database in MOVES-Matrix consists of an array of emission rates at multiple levels that resulted by running several iterative MOVES runs. Users can apply scripting techniques to model emissions for every link, in this case every work zone principal area, in the transportation network (*21 and 28*). To save processing time, a matrix table for emission rates in grams per hour was obtained for each operating mode instead of running the model for each work zone principal area and classification. This approach was adopted from Haobing Liu et al. (*30*) where they created 23 links covering all operating mode bins for running exhaust. Each link represented 100 percent of vehicle operation for a specific bin, hence traffic volume,

length and average speed were scaled to one hour of vehicle operation. For the purpose of this analysis, emission rates from Buffalo, NY will be applied in a case study. The details of the scenario include:

- Calendar year: 2017

- Region: Buffalo, NY

- Transportation links: 23 links to represent all operating mode bins

- Source type distribution: only passenger cars are considered in the analysis (Source Type ID=21)

- Age distribution: 2017 national default age distribution from MOVES2014 (*29*) to account for fleet distribution in the U.S.

- Meteorology: average values for 2017 summer months, i.e. between May and September

    - Average temperature (in 5°F increment): 70°F

    - Average relative humidity (in 5% increment): 75%

The analysis in this paper focused on comparing emissions for CO, NOx, PM2.5 and CO_2. Majority of HC emissions are highly correlated with vehicle cold starts and fuel evaporation. PM2.5 is linearly related to PM10, the same applies to the relationship between CO_2 and fuel consumption (*30*). Table 6 describes the different vehicle operating modes while Table 7 represents the emission rates (grams/hour) for each pollutant.

Table 6. Definition of Operating Modes in MOVES

OpMode Bin ID	OpMode Description	VSP (kW/metric ton)	Vehicle Speed (v_t, mph)	Vehicle Acceleration (a, mph/sec)
0	Deceleration/Braking			$a_t \leq -2.0$ OR ($a_t < -1.0$ and $a_{t-1} < -1.0$ and $a_{t-2} < -1.0$)
1	Idle		$-1.0 \leq v_t < 1.0$	
11	Coast	$VSP_t < 0$	$1 \leq v_t < 25$	
12	Cruise/Acceleration	$0 \leq VSP_t < 3$	$1 \leq v_t < 25$	
13	Cruise/Acceleration	$3 \leq VSP_t < 6$	$1 \leq v_t < 25$	
14	Cruise/Acceleration	$6 \leq VSP_t < 9$	$1 \leq v_t < 25$	
15	Cruise/Acceleration	$9 \leq VSP_t < 12$	$1 \leq v_t < 25$	
16	Cruise/Acceleration	$12 \leq VSP_t$	$1 \leq v_t < 25$	
21	Coast	$VSP_t < 0$	$25 \leq v_t < 50$	
22	Cruise/Acceleration	$0 \leq VSP_t < 3$	$25 \leq v_t < 50$	
23	Cruise/Acceleration	$3 \leq VSP_t < 6$	$25 \leq v_t < 50$	
24	Cruise/Acceleration	$6 \leq VSP_t < 9$	$25 \leq v_t < 50$	
25	Cruise/Acceleration	$9 \leq VSP_t < 12$	$25 \leq v_t < 50$	
27	Cruise/Acceleration	$12 \leq VSP_t < 18$	$25 \leq v_t < 50$	
28	Cruise/Acceleration	$18 \leq VSP_t < 24$	$25 \leq v_t < 50$	
29	Cruise/Acceleration	$24 \leq VSP_t < 30$	$25 \leq v_t < 50$	
30	Cruise/Acceleration	$30 \leq VSP_t$	$25 \leq v_t < 50$	
33	Cruise/Acceleration	$VSP_t < 6$	$50 \leq v_t$	
35	Cruise/Acceleration	$6 \leq VSP_t < 12$	$50 \leq v_t$	
37	Cruise/Acceleration	$12 \leq VSP_t < 18$	$50 \leq v_t$	
38	Cruise/Acceleration	$18 \leq VSP_t < 24$	$50 \leq v_t$	
39	Cruise/Acceleration	$24 \leq VSP_t < 30$	$50 \leq v_t$	
40	Cruise/Acceleration	$30 \leq VSP_t$	$50 \leq v_t$	

Table 7. Running Exhaust Emission Rates from MOVES-Matrix

OpMode Bin ID	Emissions Rate (gram/hour)			
	CO	**NOx**	**PM 2.5**	**CO_2 Equivalent**
0	10.082	0.535	0.054	3375
1	7.122	0.677	0.046	3107
11	24.163	0.872	0.048	4851
12	39.860	1.706	0.055	6629
13	44.347	3.588	0.082	9257
14	63.847	6.296	0.090	11727
15	84.776	9.489	0.105	14035
16	126.995	14.684	0.304	17039
21	35.191	2.090	0.087	6520
22	43.325	2.582	0.104	7452
23	55.841	3.937	0.087	9123
24	81.936	6.708	0.099	11714
25	92.179	9.435	0.131	15520
27	144.219	15.388	0.214	20391
28	278.742	25.089	0.769	27489
29	580.110	37.298	2.977	37659
30	1894.476	49.249	6.459	47262
33	28.348	3.004	0.174	9341
35	50.419	8.714	0.207	14899
37	71.249	12.654	0.198	19368
38	248.919	20.768	0.400	25253
39	295.506	29.878	0.914	33626
40	829.805	37.730	1.055	42845

Results and Discussion

The results in terms of speed-acceleration distributions, VSP distributions and total emissions rate per mile are discussed in this section.

Speed-Acceleration Plots

The acceleration and speed kernel density plots in Figures 3 through 5 show the changes in vehicle activity for the three work configuration categories as drivers transition between the different work zone components. Changes in congestion level were also considered. The smooth curves were fitted using nonparametric density estimation which computed the probability density function of speed and acceleration. The following inferences can be obtained from evaluation of the plots:

- Across the three different work zone configurations, the distribution of acceleration and deceleration are almost symmetrical which can be attributed to the fact that there are constant changes in driver behavior. The variation in acceleration is low for non-congested flow at baseline conditions as drivers are operating at higher speeds. When vehicles transition from upstream section of the highway and enter the vicinity of a work zone, lower speeds are noticed with more variability in acceleration. This is expected since drivers have been informed about upcoming roadway construction activity and are advised to lower their speeds using regulatory signs. In addition, as traffic flow becomes more restricted and a queue forms before entering the activity area, drivers travel at lower speeds and higher acceleration/deceleration rate. More braking accompanied by acceleration is induced for congested flow conditions inside work zones.

- The density plots illustrate that vehicles travel within the same speed range in advanced warning area when compared to the baseline condition unless there is high traffic density. However, the range of speed and acceleration increases as vehicles transition to the activity area.

- Lane closure and complex work zone configurations have similar acceleration and speed plots. It can also be observed that the lowest speeds and highest acceleration/deceleration rates occur in the advanced warning area for highly congested traffic flows while there is more variation in speed in the activity area. Congestion level for each trace is determined from forward videos before the

driver entered the activity area. In most cases, the formation of a queue started in the advanced warning area and it dissipated inside the activity area.

- For shoulder closure, there is a wide variation in speed and acceleration for highly congested traffic flow condition across all work zone components with more skewness towards higher speeds. This is because slower speeds are not needed in most shoulder closure situations, hence drivers tend to continue traveling at higher speeds. However, when traffic density increases, there are more changes in acceleration/deceleration rate.

Figure 3. Acceleration and speed distribution for shoulder closure zone configuration comparing different congestion level and principal areas.
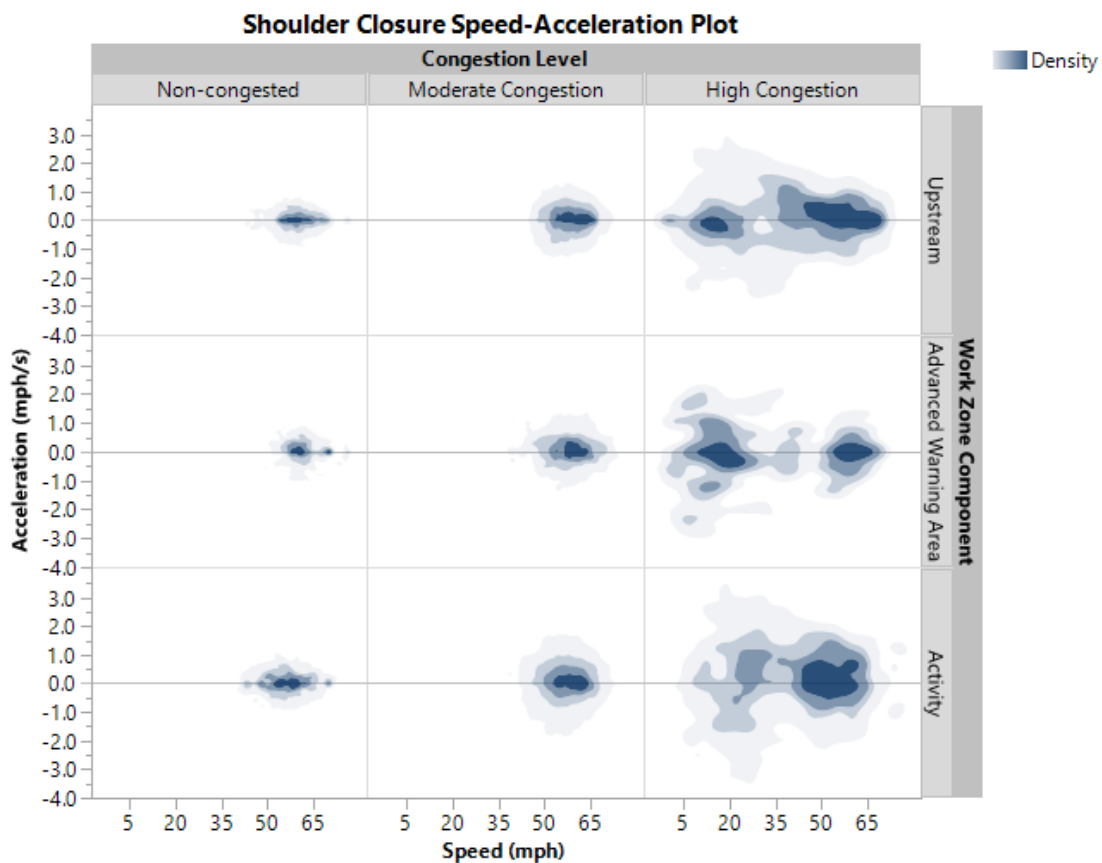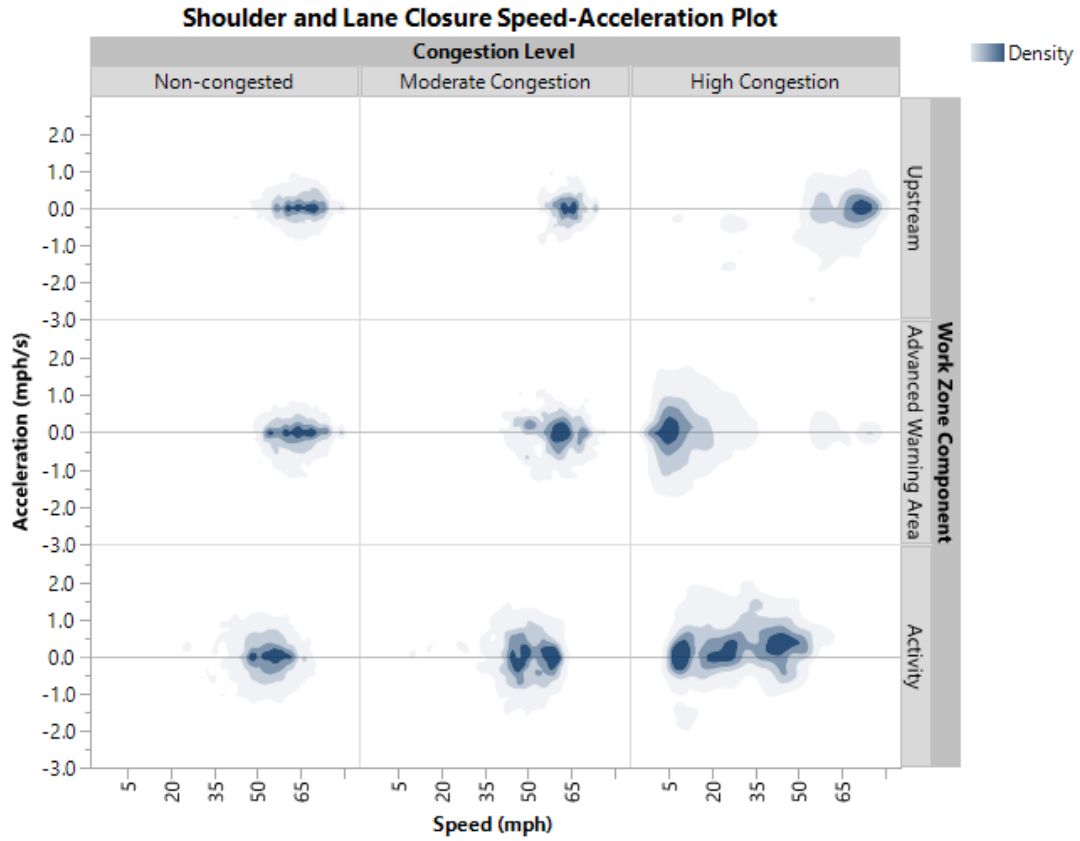
Figure 4. Acceleration and speed distribution for shoulder and lane closure zone configuration comparing different congestion level and principal areas.
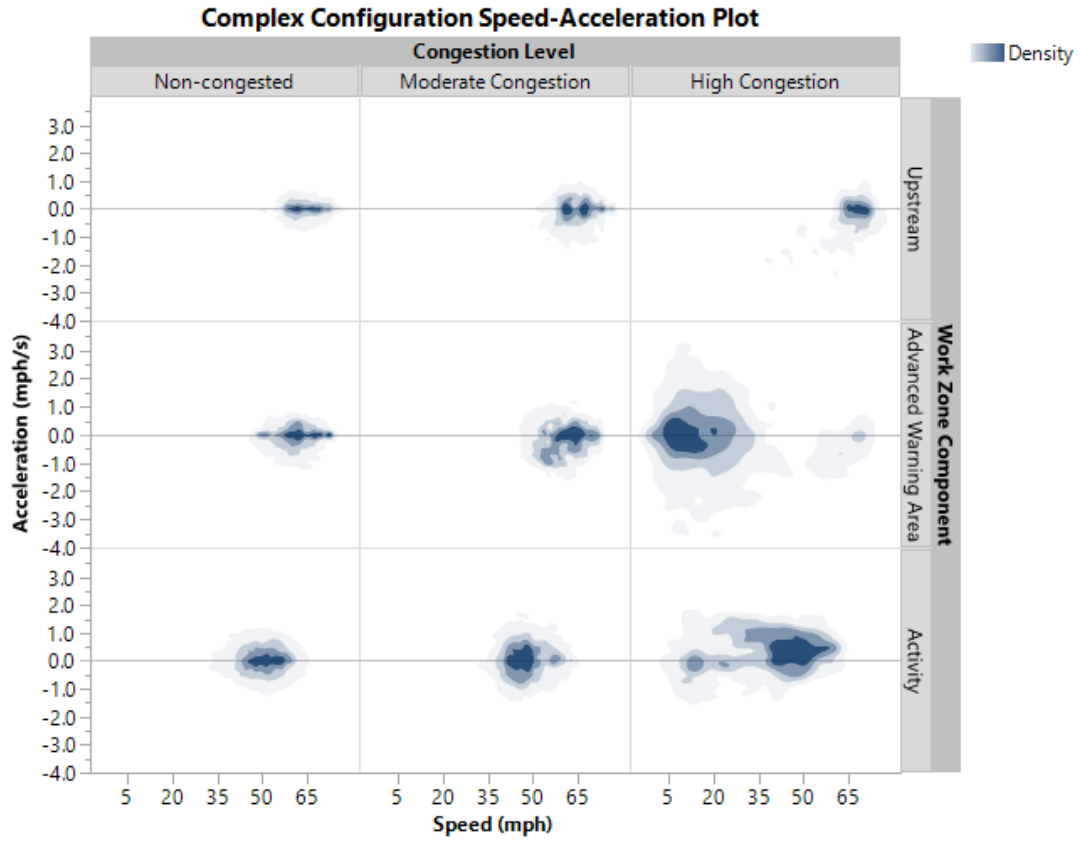
Figure 5. Acceleration and speed distribution for complex work zone configuration comparing different congestion level and principal areas.

VSP Distribution

The stacked area plot in Figure 6 shows the VSP distribution for the different work zone configurations and congestion level. VSP is an effective measure of engine load accounting for changes in vehicle activity which is correlated to emissions. It is binned in such a way that three main vehicle operations are represented: deceleration (VSP<0), idling (0≤VSP<1) and cruising/acceleration (VSP>1). Higher emission rates and fuel consumption (per second) are associated with higher VSP bins. VSP distribution tends to shift to higher modes/bins when vehicles are traveling at higher speeds, or accelerate hard at moderate to high speeds. According to the plot, for all work zone configurations, majority of VSP distribution for non-congested and moderately congested traffic flow conditions in the upstream section and advanced warning area of a work zone ranges between 7 and 19 kW/ton. Whereas, the activity area shifts the VSP to lower bins, between 1 and 10 kW/ton. The frequency of VSP in deceleration and idling vehicle operating modes increases as the traffic stream becomes highly congested. This is mostly evident in the advanced warning area. As mentioned previously, vehicles started to queue before a vehicle entered a construction zone for most trips but the queue dissipated within the activity area. As a result, the frequency of VSP is higher in the lower bins for the activity component at high congestion level.
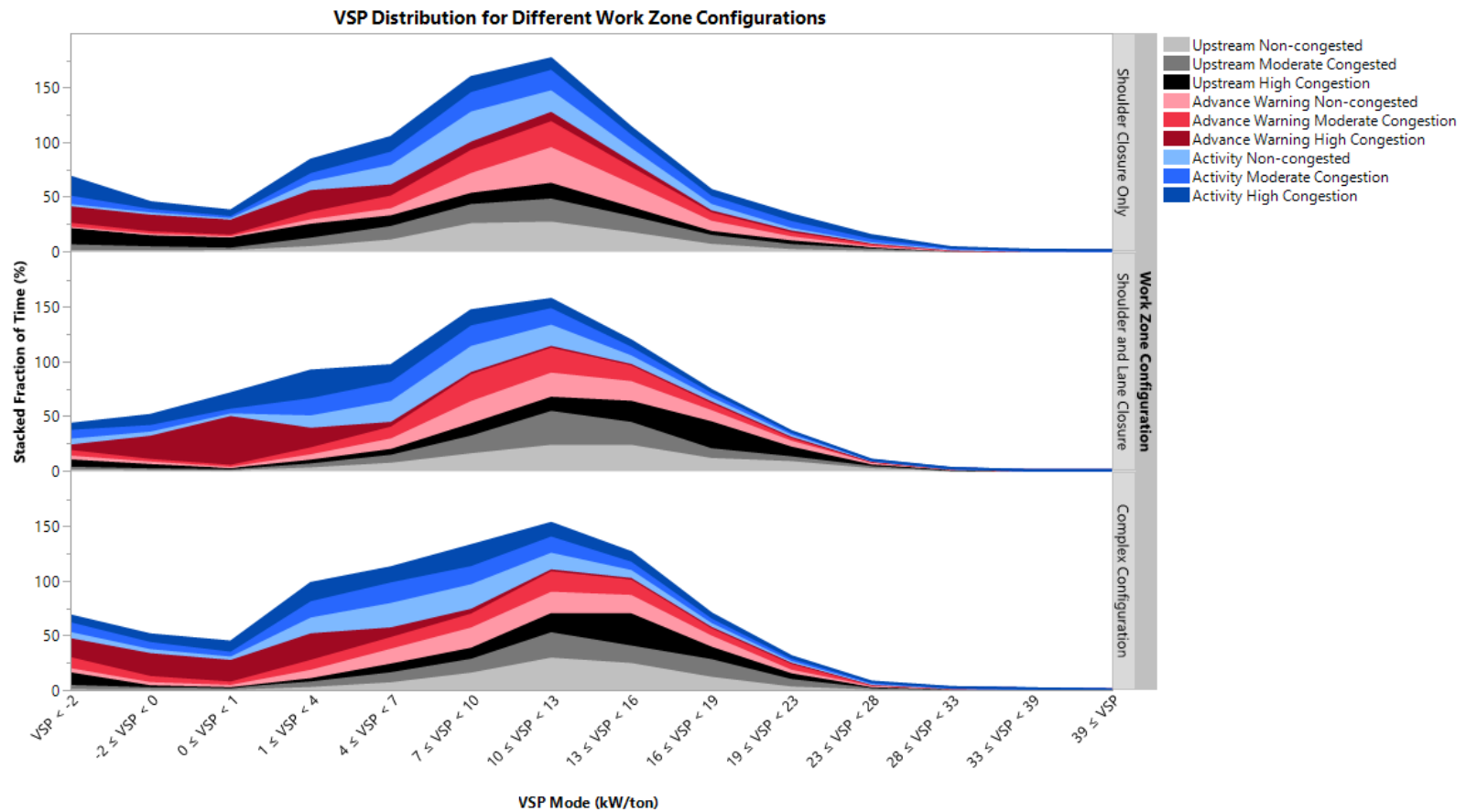
Figure 6. Stacked VSP distribution across all different work zone configurations and congestion level.

Emissions Comparison

Buffalo, NY is used as a case study to obtain emission factors for CO, NOx, PM2.5 and CO_2 by running MOVES-Matrix at project-level for 2017 calendar year. The factors are assigned to every second of data based on operating mode distribution then the product is summed to find total emissions. Figures 7 through 10 represent average emission rates per mile for the various work zone principal areas and configurations, including congestion level. There is lack of sufficient evidence indicating that there are differences in emission rates when comparing work zone principal area and configuration. On the other hand, congestion level affected emission rates and this is mostly evident in the activity portion of the work zone. There is more variability in emission rates for high congestion levels due to the high changes in speed and acceleration. More traces are needed to explore any major differences between area type, configuration and congestion level.

Figure 7. CO emission rate per mile for different work zone configurations and congestion level.

Figure 8. NOx emission rate per mile for different work zone configurations and congestion level.

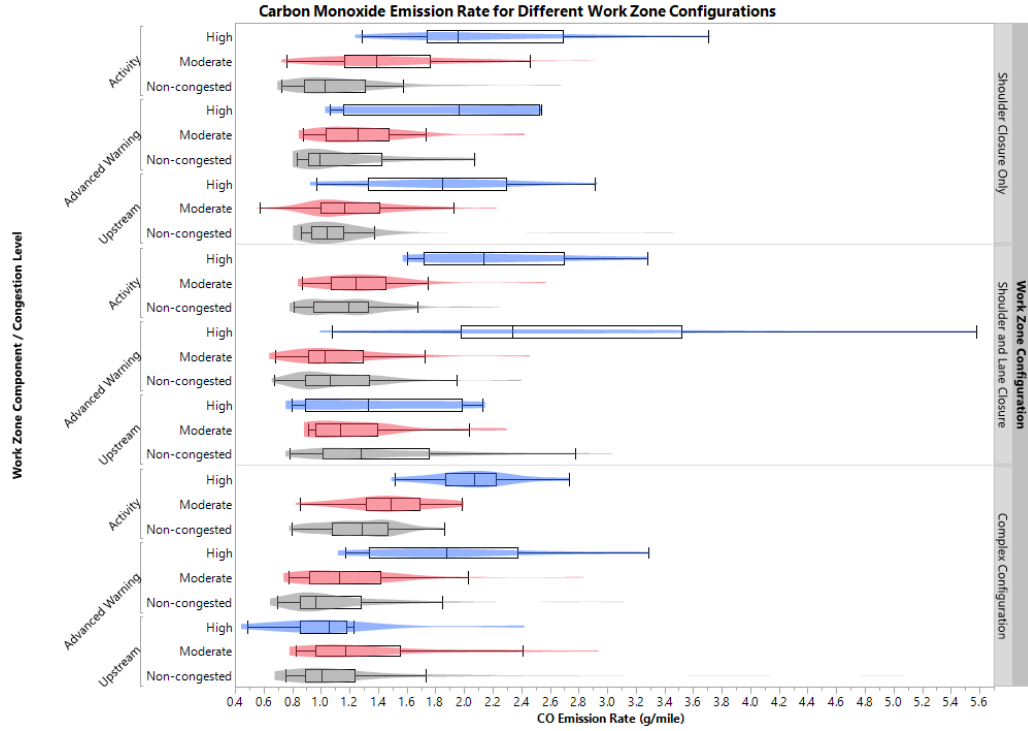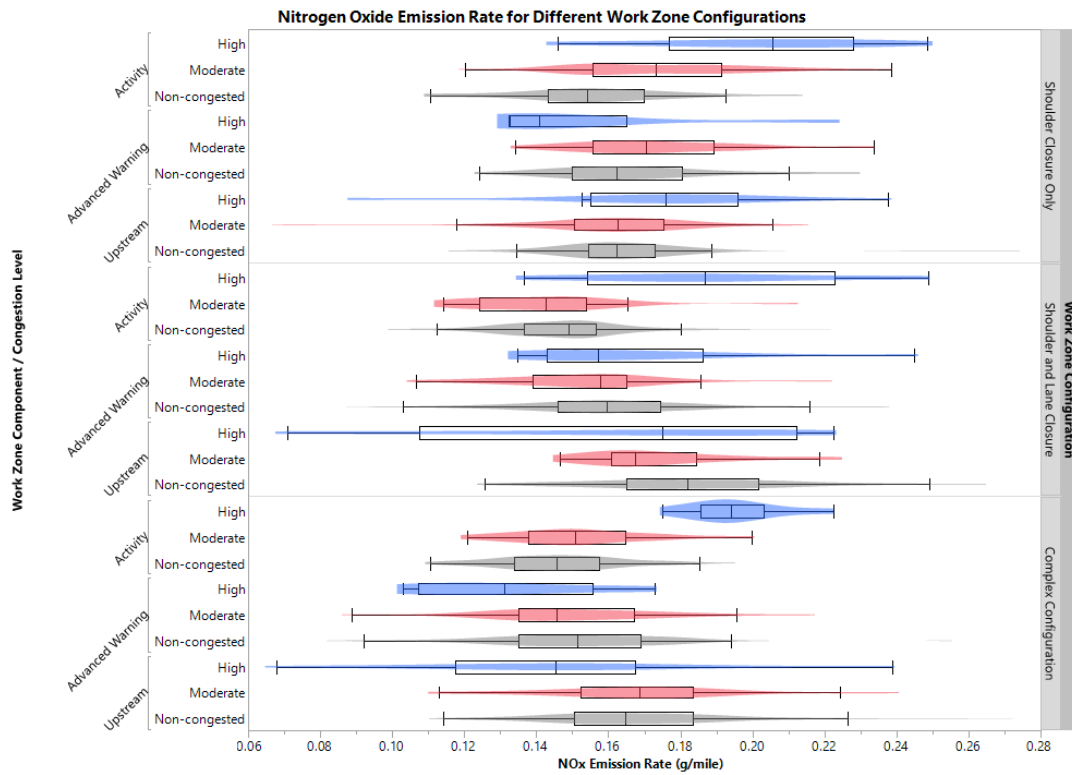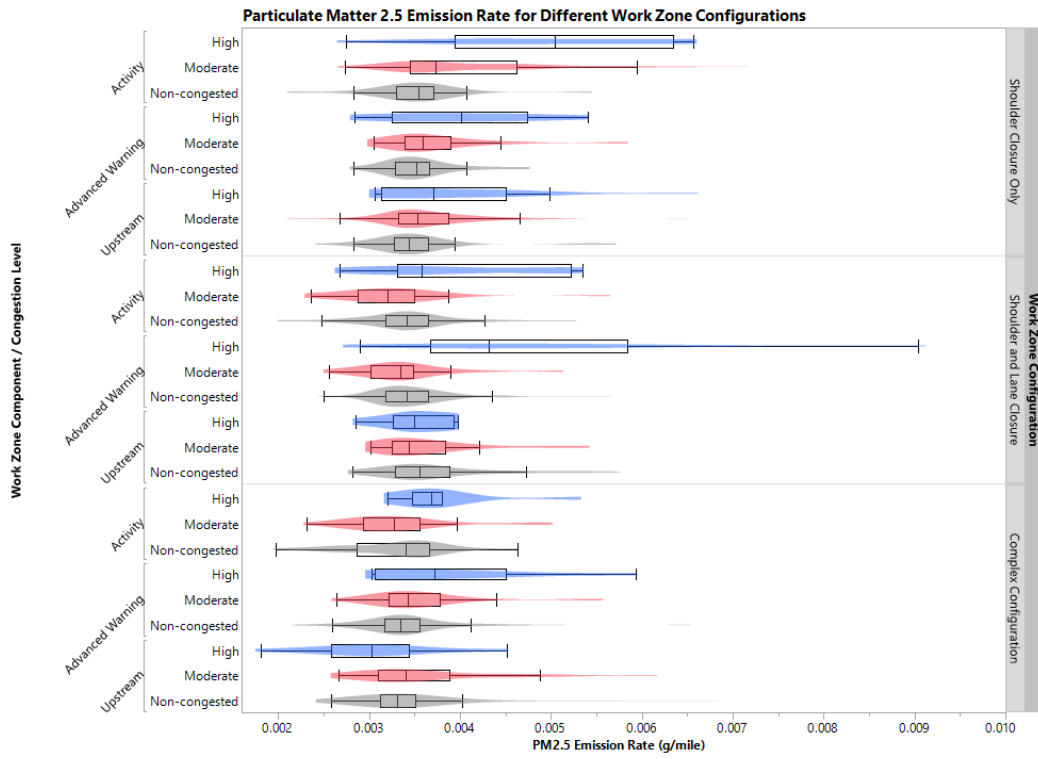**Figure 9. PM2.5 emission rate per mile for different work zone configurations and congestion level.**
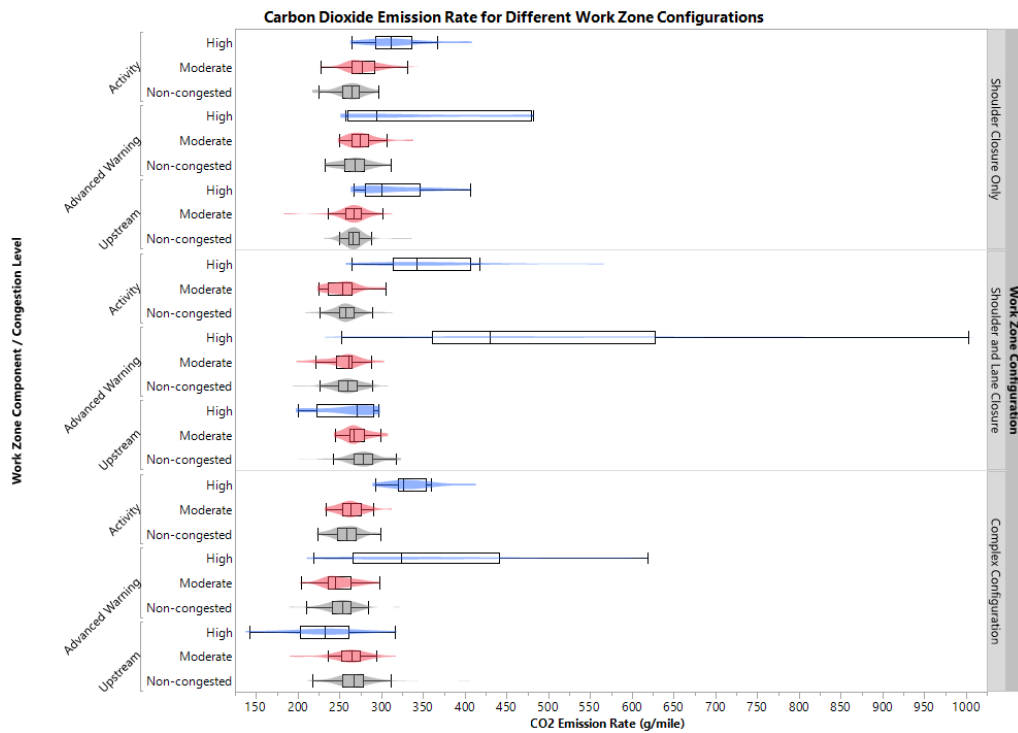

Figure 10. CO₂ emission rate per mile for different work zone configurations and congestion level.

Energy of Data: Application of Energy-Statistics to Compare 2-Sample Bivariate Vehicle Kinematics for Equality in Distributions

Emission of air pollutants from vehicles are variable due to changes in vehicle technology, vehicle operation on different roadway types, fuel specifications and quality, ambient meteorological conditions, as well as vehicle mileage accumulation (*31*). Estimating emissions using the operating mode distribution methodology basically assigns an emission factor to each second of data which relies on instantaneous vehicle kinematics in terms of speed and acceleration. Emissions analysis of various pollutants for the different work zone categories indicated that higher congestion level increased emissions. Even though it is impractical to assert that work zone configuration and principal area had a major impact on emission rate, the kernel density speed and acceleration plots disclose a different narrative. The shaded contours representing the density of the data points in Figures 3 through 5 illustrate that there are dissimilarities in the operation of vehicles while traveling through the different work zone configurations and principal components at varying traffic density. Subsequently, it is rational to investigate if the differences in vehicle kinematics are statistically significant. Previously, Hallmark and Guensler (*32*) compared 3-dimensional speed and acceleration profiles from field measurements to output from NETSIM traffic simulation software at signalized intersections. The intent of the study was to determine if the instantaneous modal vehicle activity outputs from the simulation adequately represented the field data. However, the only metric used to assess these frequency plots was to compute the percent of time vehicles spent in binned speed and acceleration ranges. Information tends to be lost when data is aggregated or binned (*33*). In recent years, a new non-parametric

binning-free goodness-of fit test for equality of two or more multivariate distributions was proposed (*34 and 35*). The statistical model, known as the energy test is practical and powerful when multidimensional data points are compared to check if the samples belong to the same parent distribution (*36*). Therefore, this test will be used to evaluate the different bivariate speed and acceleration distributions.

The development of the energy-statistics eliminates ordering and binning of data to test for equal distribution in high dimensions. It is a multivariate non-parametric test, which means that it does compare the distributions of the samples without forcing a specific shape. The test is a function of the Euclidean distance between observed samples in the variate space (*34 and 37*) and the value of the energy-statistics is an indication of the potential energy of the data for a given data set. This concept was adapted from the notion of Newton's gravitational potential energy between two bodies (*37*). One-dimensional data comparisons based on the empirical distribution functions have been extensively studied in the past with the application of well-known non-parametric tests such as Kolmogorov-Smirnov (KS) and Cramer-von Mises (CM). However, certain issues might emerge when using the KS and other cumulative tests to perform goodness-of-fit comparisons of multidimensional data. These statistical methods would depend on ordering of the data to obtain the cumulative distribution functions which results in large number of possible ways to order the data in a multidimensional space (35 *and 36*). In addition, the energy test does not make any assumptions regarding the continuity of the underlying distributions of the samples. Therefore, it is considered to be more generalized in comparison to the tests which are based on ranks of neighbors.

Suppose that $X_1, \ldots, X_{n1}$ and $Y_1, \ldots, Y_{n2}$ are independent random samples of

random vectors with respective distributions F_1 and F_2. The two-sample energy (ε) test

statistics for equal distribution consists of three terms corresponding to the energy of each

random sample X (ε_X) and Y (ε_Y) along with the interaction energy of the two samples

(ε_{XY}) (38). Therefore, the two-sample test statistic is equivalent to (35):

$$\varepsilon_{n1,n2} = \varepsilon_X + \varepsilon_Y + \varepsilon_{XY}, \text{ and} \tag{2}$$

$$\varepsilon_{n1,n2} = \frac{n_1 n_2}{n_1 + n_2} \left(\frac{2}{n_1 n_2} \sum_{i=1}^{n_1} \sum_{m=1}^{n_2} ||X_i - Y_m|| - \frac{1}{n_1^2} \sum_{i=1}^{n_1} \sum_{j=1}^{n_2} ||X_i - X_j|| - \frac{1}{n_2^2} \sum_{l=1}^{n_1} \sum_{m=1}^{n_2} ||Y_l - Y_m|| \right)$$

Where, n is the total sample size of the pooled sample. Under the null

hypothesis, $H_0: F_1 = F_2$ a random permutation of the pooled sample is equal in

distribution to a random sample size n. In other words, the two samples are equal in

distribution. In the composite alternative, the null hypothesis is rejected when $H_1: F_1 \neq$

F_2. Typically, larger values of the ε-statistics are significant (35).

When considering the bivariate speed and acceleration distributions that are

generated for the purpose of this research project, there are three main work zone

configurations. For each configuration, the work zone is divided into three principal

components and there are three categories for the traffic density. Consequently, this

results in 27 speed and acceleration distributions. If two distributions are compared at a

time without repetition and the order of selection is not a major concern, then a total of

351 combinations are produced. The multi-sample energy test of equal distribution,

eqdist.etest function, from the 'energy' package in R (39) is used to compare all 351

combinations. Results from the two-sample energy test for all the combinations implied

that the 27 bivariate vehicle kinematic distributions are significantly different. The p-value for the ε-statistics for the 351 samples/combinations is less than 0.005, hence there is strong evidence that there are differences in the distributions. The relative scale of speed and acceleration are not the same which might result in one of the projections dominating the value of the energy while the other projection only marginally contributing to it. However, the Euclidean distance between observations is normalized in the ε-statistics.

Conclusion

This study evaluated a new potential data source to model emissions from passenger cars at the project-level for work zones on freeway roadway segments. Conclusions of the tasks completed as part of this study are summarized as follow:

- Previous studies proved that there is a correlation between vehicle engine load and exhaust emissions. Therefore, it is possible to estimate emissions with increased precision using disaggregate vehicle kinematics data.

- Only few researchers quantified emissions at work zones because designing an experiment to collect field observations requires funding and resources.

- SHRP2 NDS is a potential source of data in emissions modeling since the study recorded various attributes at the microscopic (second-by-second) level.

- Work zones on four-lane divided principal arterials were analyzed to examine differences in vehicular emissions for different work zone configurations and level of congestion.

- A total of 532 traces from 45 unique work zone locations were coded. The traces were represented from three different states across the U.S., New York, Pennsylvania and Washington.

- Comparative analysis using box-plots showed that only congestion level had an impact on emissions rate per mile. Errors from second-by-second VSP computations might be eliminated when aggregating total emissions. This is because emissions are a function of various factors. As a result, it was necessary to examine the instantaneous speed and acceleration input data.

- A non-parametric goodness-of-fit statistical test, known as energy statistics, was applied to compare the different kernel density speed and acceleration distributions. Results implied that the work zone configuration and principal component also had a significant impact on vehicle operations.

- More traces can be reduced in the future to distinguish any differences in emissions across the different work zone configurations.

References

1. Work Zone Management Program. *Facts and Statistics – Work Zone Mobility*. Office of Operation, Federal Highway Administration (FHWA). https://ops.fhwa.dot.gov/wz/resources/facts_stats/mobility.htm. Accessed November 15, 2017.

2. Tanvir, S., N. M. Rouphail and B. J. Schroeder. Network Level Impacts of Major Freeway Reconstruction Project on Vehicular Emission. Presented at Air and Waste Management Association (AWMA) 108th Annual Conference and Exhibition, Raleigh, North Carolina, 2015.

3. Zhang, K., S. Batterman and F. Dion. Vehicle Emissions in Congestion: Comparison of Work Zone, Rush Hour and Free-flow Conditions. *Atmospheric Environmental Journal*, Vol. 45, 2011, pp. 1929 – 1939.

4. Salem, O., S. Pirzadeh, S. Ghorai and A. Abdel-Rahim. Improving Sustainability of Work-zones by Implementing Lean Construction Techniques. Presented at

International Conference on Architecture and Civil Engineering (ICAACE), Dubai, U.A.E, 2014.

5. Qiao, F. J. Jia, L. Yu, Q. Li and D. Zhai. Drivers' Smart Assistance System Based on Radio Frequency Identification: Enhanced Safety and Reduced Emissions in Work Zones. *Transportation Research Record: Journal of Transportation Research Board*, No. 2458, 2014, pp. 37 – 46.

6. Li, Q., F. Qiao, X. Wang and L. Yu. Measures of Performance When Drivers Approaching STOP Sign Intersections with the Presence of Drivers' Smart Advisory System. Presented at 28th Annual Conference of the International Chinese Transportation Professionals Association (ICTPA), Los Angeles, California, 2015.

7. Li, Q., F. Qiao and L. Yu. Vehicle Emission Implications of Drivers' Smart Advisory System for Traffic Operations in Work Zones. *Journal of AWMA*, Vol. 6, No. 5, 2016, pp. 446-455.

8. Zhou, X., S. Tanvir, H. Lei, J. Taylor, B. Liu, N. M. Rouphail and H. C. Frey. Integrating a Simplified Emission Estimation Model and Mesoscopic Dynamic Traffic Simulator to Efficiently Evaluate Emission Impacts of Traffic Management Strategies. *Transportation Research Part D Journal*, Vol. 37, 2015, pp. 123 – 136.

9. Farzaneh, R., et al. *Air Quality Benefits of Nighttime Construction in Texas Non-Attainment Counties: Technical Report*. Publication FHWA/TX-17/0-6864-1. Texas Transportation Institute (TTI), Texas A&M University, College Station, Texas, 2017.

10. Thomas, S. Modeling of Freeway Air Quality during Recurring and Nonrecurring Congestion Events. Ph.D. Dissertation, Purdue University, West Lafayette, Indiana, 2007.

11. Barth, M. and K. Boriboonsomsin. Real-World Carbon Dioxide Impacts of Traffic Congestion. *Transportation Research Record: Journal of Transportation Research Board*, No. 2058, 2008, pp. 163 – 171.

12. Bigazzi, A. Y. and M. Figliozzi. An Analysis of the Relative Efficiency of Freeway Congestion Mitigation as an Emission Reduction Strategy. Presented at the 90th Annual Meeting of the Transportation Research Board, Washington, D.C., 2011.

13. Papson, A., S. Hartley and K.L. Kuo. Analysis of Emissions at Congested and Uncongested Intersections with Motor Vehicle Emission Simulation 2010. *Transportation Research Record: Journal of Transportation Research Board*, No. 2270, 2012, pp. 124 – 131.

14. Qi, Y., A. Padiath, Q. Zhao and L. Yu. Development of Operating Mode Distributions for Different Types of Roadways under Different Congestion Levels for Vehicle Emission Assessment using MOVES. *Journal of AWMA*, Vol. 66, No. 10, 2016, pp. 1003 – 1011.

15. Hankey, J. M., J.A. McClafferty, M. A. Perez. *Description of the SHRP2 Naturalistic Database and the Crash, Near-Crash, and Baseline Data Sets*. Virginia Tech Transportation Institute, Blacksburg, Virginia, 2016.

16. Sun, Y., H. Xu, J. Wu, E. Hajj and X. Geng. Data Processing Framework for Driving Cycle Development with Naturalistic Driving Study Data. *Transportation Research Record: Journal of Transportation Research Board*, No. 2645, 2017, pp. 50 – 56.

17. Farzaneh et al. *Texas-Specific Drive Cycles and Idle Emissions Rates for Using with EPA's MOVES Model*. FHWA/TX-14/0-6629-1. Texas Transportation Institute (TTI), Texas A&M University, College Station, Texas, 2014.

18. Liu, Z., A. Ivanco, Z. Filipi. Naturalistic Drive Cycle Synthesis for Pickup Trucks. *Journal of Safety Research*, Vol. 54, 2015, pp. 109 – 115.

19. LeBlanc, D. J., M. Sivak and S. Bogard. *Using Naturalistic Driving Study Data to Assess Variations in Fuel Efficiency among Individual Drivers.* Publication UMTRI-2010-34. Transportation Research Institute, University of Michigan, Ann Arbor, Michigan, 2010.

20. Tanvir, S., T. Chase and N. M. Rouphail. Heterogeneity and Consistency of Eco-Driving Metrics Using Naturalistic Driving Data. Presented at the 96th Annual Meeting of the Transportation Research Board, Washington, D.C., 2017.

21. Abou-Senna, H., E. Radwan, K. Westerlund and C. D. Cooper. Using a Traffic Simulation Traffic (VISSIM) with an Emission Model (MOVES) to Predict Emissions from Vehicles on a Limited-Access Highway. *Journal of AWMA*, Vol. 63, No. 7, 2013, pp. 819 – 831.

22. Guensler, R., H. Liu, X. Xu, Y. Xu and M.O. Rodgers. MOVES-Matrix: Setup, Implementation and Application. Presented at the 95th Annual Meeting of the Transportation Research Board, Washington, D.C., 2016.

23. Hallmark, S., A. Goswamy, O. Smadi and S. Chrysler. Speed Prediction in Work Zones Using the SHRP2 Naturalistic Driving Study Data. Presented at the 10th SHRP2 Safety Data Symposium, Washington, D.C., 2017.

24. Part 6: Temporary Traffic Control. In *Manual on Uniform Traffic Control Devices*. FHWA, U.S. Department of Transportation, 2009, pp. 547 – 730.

25. *SHRP2 Researcher Dictionary for Video Reduction Data Version 4.1*. Virginia Tech Transportation Institute, Blacksburg, Virginia.

https://vtechworks.lib.vt.edu/bitstream/handle/10919/56719/V4.1_ResearcherDict
ionary_for_VideoReductionData_COMPLETE_Oct2015_10-5-
15.pdf;sequence=1. Accessed July 1, 2018.

26. Frey, H. C., N. M. Rouphail, H. Zhai, T. L. Farias and G. A. Goncalves.
Comparing Real-World Fuel Consumption for Diesel- and Hydrogen-Fueled
Transit Buses and Implication for Emissions. *Transportation Research Part D
Journal*, Vol. 12, 2007, pp. 281 – 291.

27. U.S. Environmental Protection Agency. *Development of Emission Rates for Light-
Duty Vehicles in the Motor Vehicle Emissions Simulator MOVES2010*. EPA-420-
R-11-011. http://www.epa.gov/otaq/models/moves/documents/42r11011.pdf.
Accessed August 3, 2018.

28. Guensler, R., H. Liu, Y. Xu, A. Akanser, D. Kim, M. Hunter and M.O. Rodgers.
Energy Consumption and Emission Modeling of Individual Vehicles Using
MOVES-Matrix. *Transportation Research Record: Journal of Transportation
Research Board*, No. 2627, 2017, pp. 93 – 102.

29. Default Age Distribution for MOVES2014.
http://www.epa.gov/OMSmodels/moves/documents/default-age-distribution-tool-
moves2014.xlsx. Accessed August 15, 2018.

30. Liu, H., D. Sonntag, D. Brzezinski, C. R. Fulper, D. Hawkins and J. E. Warila.
Operations and Emissions Characteristics of Light-Duty Vehicles and Ramps.
Transportation Research Record: Journal of Transportation Research Board, No.
2570, 2016, pp. 1 – 11.

31. Cai, H., A. Burnham and M. Wang. *Updated Emission Factors of Air Pollutants
from Vehicle Operations in GREET^{TM} Using MOVES*. Systems Assessment
Section. Energy Systems Division. Argonne National Laboratory, 2013.

32. Hallmark, S. and R. Guensler. Comparison of Speed-Acceleration Profiles from
Field Data with NETSIM Output for Modal Air Quality Analysis of Signalized
Intersections. *Transportation Research Record: Journal of Transportation
Research Board*, No. 1664, 1999, pp. 40 – 46.

33. D. N. Schreiber-Gregory. *Data Quality Control: Using High Performance
Binning to Prevent Information Loss*. SAS Global Forum Proceedings 2018.
Paper No. 2821. https://www.sas.com/content/dam/SAS/support/en/sas-global-
forum-proceedings/2018/2821-2018.pdf. Accessed December 16, 2018.

34. Aslan, B. and G. Zech. *A new class of binning-free, multivariate goodness-of-fit
tests: the energy tests*. arXiv e-print, Cornell University, New York.
https://arxiv.org/pdf/hep-ex/0203010.pdf. Accessed November 27, 2018.

35. Szekely, G. J. and M. L. Rizzo. *Testing for Equal Distributions in High
Dimension*. Interstate Journal. 2004.

http://interstat.statjournals.net/YEAR/2004/articles/0411005.pdf. Accessed November 27, 2018.

36. Cohen, E.O., I. D. Reid and E. Piasetzky. Implementing a 3D histogram version of the Energy-Test in ROOT. *Nuclear Instruments and Methods in Physics Research Section A: Accelerators, Spectrometers, Detectors and Associated Equipment*, Volume 828, 2016, pp. 86 – 90.

37. Szekely, G. J. and M. L. Rizzo. The Energy of Data. *Annual Review of Statistics and Its Application*, Extended Review, Volume 4, 2017, pp. 447 – 479.

38. Aslan, B. and G. Zech. *A New Test for the Multivariate Two-Sample Problem Based on the Concept of Minimum Energy*. arXiv e-print, Cornell University, New York. https://arxiv.org/pdf/math/0309164.pdf. Accessed November 27, 2018.

39. M. L. Rizzo. *E-Statistics: Multivariate Inference via the Energy of Data*. Package 'energy', Comprehensive R Archive Network, 2018. https://cran.r-project.org/web/packages/energy/energy.pdf. Accessed November 27, 2018.

CHAPTER 3. USING TRAFFIC SIMULATION MODELS FOR EMISSIONS ESTIMATION AT WORK ZONES

"Application of a Generic Calibration Guidance to Assess the Precision of Vissim to Generate Real-World Vehicle Activity and Reliable Emissions Estimates"

Authors: Georges Bou-Saab[1], Archana Venkatachalapathy[1], Shauna Hallmark[1], Omar Smadi[1], Diane Xiao[2] and Christopher Hutchinson[3]

Affiliations: [1]Iowa State University- Institute for Transportation, Ames, Iowa,

[2]Greenman-Pedersen, Inc., Manhattan, New York

[3]Terra Engineering, St. Louis, Missouri

Abstract

Existing emissions rate models require disaggregate vehicle activity data as inputs. Previous efforts relied on instrumented vehicles or chase car technique to collect field data. However, these methods are resource intensive and expensive. Other efforts used micro-simulation to obtain data but various driver behavior and lane changing parameters must calibrated. This is required in order to validate that the output from traffic simulation models can represent accurate real-world driving activity. This research investigated the capability of traffic microsimulation tools to replicate field conditions to accurately estimate vehicle emissions at work zones. Vissim was used to simulate different lane closure scenarios in a case study, i.e. AM-peak hour, PM-peak hour and

nighttime off-peak lane closure. and results were compared to the SHRP2 NDS findings. Findings showed that it was necessary to calibrate the Vissim model. Consequently, a generic guidance for calibrating capacity at work zones was applied in this project to evaluate the ability of Vissim to replicate field conditions. For all the roadway construction scenarios, results showed that the Wiedemann car-following model in Vissim produced highly variable VSP and acceleration distributions relative to the field observations from SHRP2 publication.

Key Words: Emissions Estimation, Field Observations, Traffic Microsimulation, Vehicle Specific Power, Acceleration Distribution, Speed Bins

Introduction

Existing infrastructure in the United States (U.S.) has witnessed a rapid growth in rehabilitation and reconstruction projects attributable to the increasing travel demand and aging assets (*1*). Quantifying the adversity of setting up work zones allow policymakers to formulate mitigation measures, apply proposed strategies and monitor their performance. Therefore, the task of planning and managing work zones is becoming more intricate. Additionally, taking into account that local and state transportation agencies are still required to meet the safety, mobility and welfare needs of the public during roadway construction, they have to comprehend the effects of work zones on a particular transportation network.

Increasingly, more emphasis has been assigned towards providing better mobility to residents and businesses on urban roads in the U.S., whereas apprehensions for secondary user elements including congestion, crashes and air emissions are still persistent. Estimating the costs and benefits of congestion and crashes using cost-benefit

analysis (CBA) are well-documented (*2*) but there is an ongoing criticism with the use of

this technique to monetize environmental and social elements (*3*). It is a difficult task to

estimate the cost of air pollution from transportation sources since there is lack of reliable

methods that can precisely identify and quantify the origins of existing air pollution

levels (*4*). In a study to analyze the bearing of valuing greenhouse gas emissions and

errors in transportation CBA, Meunier and Quinet (*5*) determined that uncertainty can

significantly impact the assessment of physical quantities of CO_2. Therefore, these errors

must be addressed while quantifying emissions. Determining the social cost factors of

emissions in air pollution is another constraint. The damage imposed by pollutants and

greenhouse gases on human health usually determines the social unit cost of emissions.

There is no consensus on assigning a monetary value to each type of pollutant because

better evaluation is needed to understand the relationship between emissions and human

health (*4*).

Regardless of the limitations in determining a standard unit cost for air pollution,

the influence of specific transportation sources at the project-level can be isolated with

precision. To evaluate different roadway construction project scenarios, the amount of

emissions from vehicles can be predicted with the application of widely acknowledged

models, such as the U.S. Environmental Protection Agency (U.S. EPA) Motor Vehicle

Emission Simulator (MOVES). Latest version of MOVES capitalizes on the ability to

accurately model emissions by considering changes in the vehicle specific power (VSP)

which is directly correlated to the vehicle operating mode (acceleration, deceleration,

cruising and idling). This implies that emission modeling is sensitive to instantaneous

vehicle kinematics as input data. Second-by-second speed and acceleration data can be

collected from the field but this is a resource intensive method. A cost-effective option to generate realistic vehicle kinematics data is using microsimulation modeling.

The FHWA recommended the utilization of modeling and simulation tools to perform work zone analysis. Guidelines are made available to ensure that agencies are effectively using the software programs to identify potential delay and select the most economical construction scenario. They can use a combination of tools to evaluate the impact of work zones and these include but are not limited to: QuickZone, Construction Analysis for Pavement Rehabilitation Strategies (CA4PRS), Dynasmart-P and Highway Capacity Manual (HCM) (*1*). Microscopic simulation is encouraged in the case of complex modeling. Users can simulate the movement of individual vehicles using car-following and lane changing theories. Vissim, Corsim, Aimsun, Paramics and Integration are some examples of well-known microscopic traffic simulators available in the market (*1, 6*). Microsimulation models must be calibrated against field data including traffic parameters, speed distributions and driver factors, to accurately represent vehicle trajectories from the field. Merely relying on default parameters will fail to validate model output which impacts emissions. Jie et al. (*7*) showed that an uncalibrated Vissim model overestimated carbon dioxide (CO_2) and nitrogen oxide (NO_x) emission by 10 percent. As a result, this project used a case study for freeway lane closure to verify the competence of Vissim to produce realistic second-by-second data.

Quantifying Work Zone Costs and Benefits

The ability to analyze the impacts of work zones will allow project managers to make well-informed and economical choices to increase benefits, i.e. less delay,

reduction in vehicular emissions, improved safety and lower user cost. As part of a research project funded by FHWA, Mallela and Sadasivam (*8*) emphasized on the concept of work zone road user cost (WZ RUC) as a measure to quantify the negative impacts of roadway construction. It can function as a surrogate economic assessment methodology in the decision-making process. WZ RUC can also be used by transportation agencies in life-cycle cost analysis (LCCA) as well as CBA to make appropriate decisions pertaining to resource allocation for improving work zone mobility and safety. Road user costs for a work zone can be classified into two components: monetized vehicle externalities and other off-site impacts. Impacts with a monetary value consist of travel time costs, vehicle operating costs, crash costs and emission costs (*8, 9*), while off-site components include noise, business and local community impacts. Typically, converting off-site factors to money value imposes a challenge since they are site-specific. Even though the factors in the aforementioned process are considered as negative impacts or disbenefits, the majority of research available in the literature (*10, 11, 12 and 13*) apply a different practice, centered on basic economic terms and principles that are commonly used in transportation CBA. Benefits are the direct positive effects of a project resulting in costs reduction, for instance, travel time reductions, vehicle operating cost savings, safety benefits and air emission reductions. These physical benefits are converted into monetary value. Another relevant element in transportation CBA is the direct agency cost of a transportation investment which is the value of the resources used in the completion of a project which includes capital costs, rehabilitation costs, annual maintenance costs and end-of-project costs. Delay, crashes and vehicle operation, i.e. user elements, can be labelled as cost or benefit depending on the outcome

of each alternative project and their effect on the users. Finally, the time value of money must be considered in any CBA by converting future costs and benefits into present value. Despite the prevalent use of CBA to compare project alternatives, there are limitations in assessing environmental and social impacts (*14, 3*). Obtaining emission rates from models require several assumptions in terms of topographical and climatic conditions of the region, vehicle properties, vehicle speed, acceleration and deceleration, fuel type and etc. Therefore, emissions estimates of each pollutant are profoundly influenced by the input values. It is also difficult to measure the effect of emissions in monetary units due to large ranges in the uncertainty of pricing (*15, 16, 17 and 18*). Deriving the unit costs of emissions depend on the economic analysis performed on the health impacts of air pollutants and greenhouse gases.

Use of Microsimulation Modeling to Assess Various Transportation Strategies

Currently, microsimulation tools are well-recognized as they can model complex transportation networks and allow users to examine different traffic incident scenarios stochastically, reflecting the dynamic distribution of traffic. They also present an alternate option to field data collection with the generation of instantaneous speed and acceleration profiles for individual vehicles (*19 – 25*). The accuracy of these systems to generate reliable vehicle activity output depends on the dynamic behavior of the vehicles in the network which is a function of the car-following, lane changing and gap acceptance models (*19 and 26*). Depending on the software utilized, the driving behavior algorithms in the simulation models are based on theoretical profiles intended to describe the overall vehicle activity (*23 and 27*). Hence, the behavioral parameters have to be calibrated and validated based on input data from the field to ensure that the models are

replicating traffic patterns that are similar to local conditions. FHWA suggested three logical and sequential calibration strategies (*28*) utilizing capacity, route-choice and overall system performance. In all cases, calibration is achieved by fine-tuning certain parameters to enable the model to better match the field measurements. Unfortunately, the task of measuring driving behavior characteristics from the field is problematic and in most cases, the available data are insufficient (*22 and 26*). Researchers and practitioners showed interest in microsimulation to precisely reproduce traffic operations on urban freeways (*22, 25, 29-34*) and analyze the impact of traffic incidents, such as congestion and work zones, on mobility (*20, 24, 35-43*). This was achieved by the development of a framework to calibrate and validate the models from field measurements on case-by-case basis. As a result of quantifying the consequences of traffic incidents, the expenditure of public funds on transportation projects can be justified.

Importance of Microsimulation Modeling in Emissions Estimation

Weighing of different real-time transportation policies and traffic management strategies, such as the implementation of work zones, is essential in the selection of scenarios which improves the overall operation of vehicles during lane closure and reduces on-road emissions (*44*). Analyzing transportation air quality in the past relied on aggregate activity measures such as average speed but this produced inaccurate emission inventories, in other words either underestimated or overestimated actual emissions. With the development of MOVES by the U.S. EPA, which is a nationally approved highway emissions rate model, users can predict differences in emissions at project-level for various roadway construction scenarios by providing site-specific inputs (*23*). MOVES takes into account the changes in vehicle operating modes or engine load, i.e. the fraction

of time vehicles spent decelerating, accelerating and idling, which requires instantaneous vehicle activity data. Such data can be collected from the field using chase cars or instrumented vehicles. Nonetheless, this is an impractical, expensive and time consuming approach. Subsequently, several researchers applied and studied the integration of traffic simulation models with vehicle emission models (*23*, *45-53*) to enhance the calculation of emissions by using second-by-second speed and acceleration profiles. Earlier efforts focused on using cumulative speed distribution and flow to calibrate and validate traffic microsimulation models. These traditional calibration methods were questioned (*21, 26, 27, 54-58*) due to the unrealistic higher cruising conditions along with hard acceleration and deceleration rates of simulated vehicles when compared to field observations. This illustrates the importance of calibrating and validating the dynamic behavior of simulated vehicles to replicate real-world driving patterns using disaggregate parameters. Recently, Song et al. (*44, 60*) and Wang et al. (*59*) explored most commonly used car-following models to test how accurately they captured vehicle dynamics for emissions estimation when compared to field measurements. In 2013, Song et al. (*44*) showed that the VSP distributions from the optimal velocity model (OVM) and generalized force model (GFM) differed largely from the field trajectories which can lead to significant errors in emissions estimates. The Wiedemann car-following model which is included in Vissim tended to create more VSP fraction peaks, especially in the aggressive driving modes. However, they demonstrated that the Fritzsche model used in Paramics software tool produced realistic VSP distributions consistent with field conditions. In another study (*60*), Song found that by optimizing both the maximum following distance and maximum acceleration profiles, the differences between the Wiedemann simulated VSP

distributions and the field can be marginally reduced. Wang et al. (*59*) validated that

Rakha-Pasumarthy-Adjerid (RPA) car-following model employed in the Integration

traffic micro-simulator yielded realistic VSP distributions when compared to other state-

of-the-practice models, namely Wiedemann, Gipps and Fritzsche models.

In many cases, it is not feasible for local agencies to collect detailed and large

amount of field data to calibrate traffic, vehicle and driver properties. Therefore, Yeom et

al. (*61*) proposed a generic framework which can be applied by researchers to calibrate

the capacity of work zones on freeways depending on lane closure configuration. As part

of NCHRP Project 03-107, field observations from 81 locations and a total of 90 work

zones across 12 U.S. states were used to develop a simulation guidance in Vissim by

adjusting particular car-following and lane changing parameters. They determined that

only cc1 and cc2 parameters in the Wiedemann 99 car-following model should be fine-

tuned to account for the lane closure configuration and replicate the average queue

discharge flow rate. The parameters defining the driver behavior in the psycho-physical

car-following model used in Vissim include:

cc0: standstill distance between two vehicles

cc1: desired headway time between lead and trailing vehicles

cc2: additional distance over desired safety distance

cc3: time in seconds to start of the deceleration process

cc4: negative speed variations during the following process

cc5: positive speed variations during the following process

cc6: influence of speed on distance oscillation

cc7: oscillation during acceleration

cc8: desired acceleration from standstill

cc9: desired acceleration at 50 mph

The researchers also recommended adjusting the lane changing parameters to demonstrate realistic work zone conditions on freeways as vehicles tend to be more cautious and change lanes at an earlier distance in comparison to non-work zone conditions. In this context, the objective of the research study is to create a Vissim microsimulation model and test the generic guidance for capacity calibration to evaluate the impact of different lane closure strategies on vehicle operations using second-by-second activity data. Outputs from Vissim will be used to compute the vehicle specific power (VSP) then perform a comparative analysis against real-world vehicle kinematics data from the Second Strategic Highway Research Program (SHRP2) Naturalistic Driving Study (NDS). Detailed exploration of the findings can determine if the Vissim guidance generates precise emissions estimates to incorporate in CBA.

Research Study Methodology

The general methodology adopted in the project is described in Figure 11. Initially, the perimeter of the study area is determined followed by the collection of existing traffic counts, speed distributions and geometric characteristics from state or local agencies. The acquisition of local data is an important step since these are used as inputs in the microsimulation. A base case model is then created in Vissim to simulate traffic flow for the existing conditions. An initialization period is added to the simulation running period to allow for the model to warm-up. Next, the model must be calibrated with respect to system performance data and experimented with at least 5 (up to 10) random seeds. This will verify if Vissim is able to replicate the conditions of the current

traffic network. The error is recommended to be within a 5 percent margin when results are compared to the actual data. Once the model is validated, the various traffic incident management scenarios can be implemented by adjusting the base case model. The different roadway closure scenarios are simulated in Vissim with default model parameters considering the base case model is initially calibrated based on volume and desired speed. Subsequently, the guidance for calibrating capacity at work zones is applied in another scenario to fine-tune the necessary default car-following and lane changing parameters. Model simulation is repeated with the new recommended parameters. Finally, outputs will be compared to field observations from instrumented vehicles in a SHRP2 study using the vehicle specific power (VSP) to evaluate the accuracy of Vissim in producing realistic speed and acceleration profiles. Therefore, this will have an impact on emissions estimates. The SHRP2 study estimated emissions from passenger cars at work zones on 4-lane divided principal arterials with different configurations. The analysis also considered work zone principal areas and level of congestion.
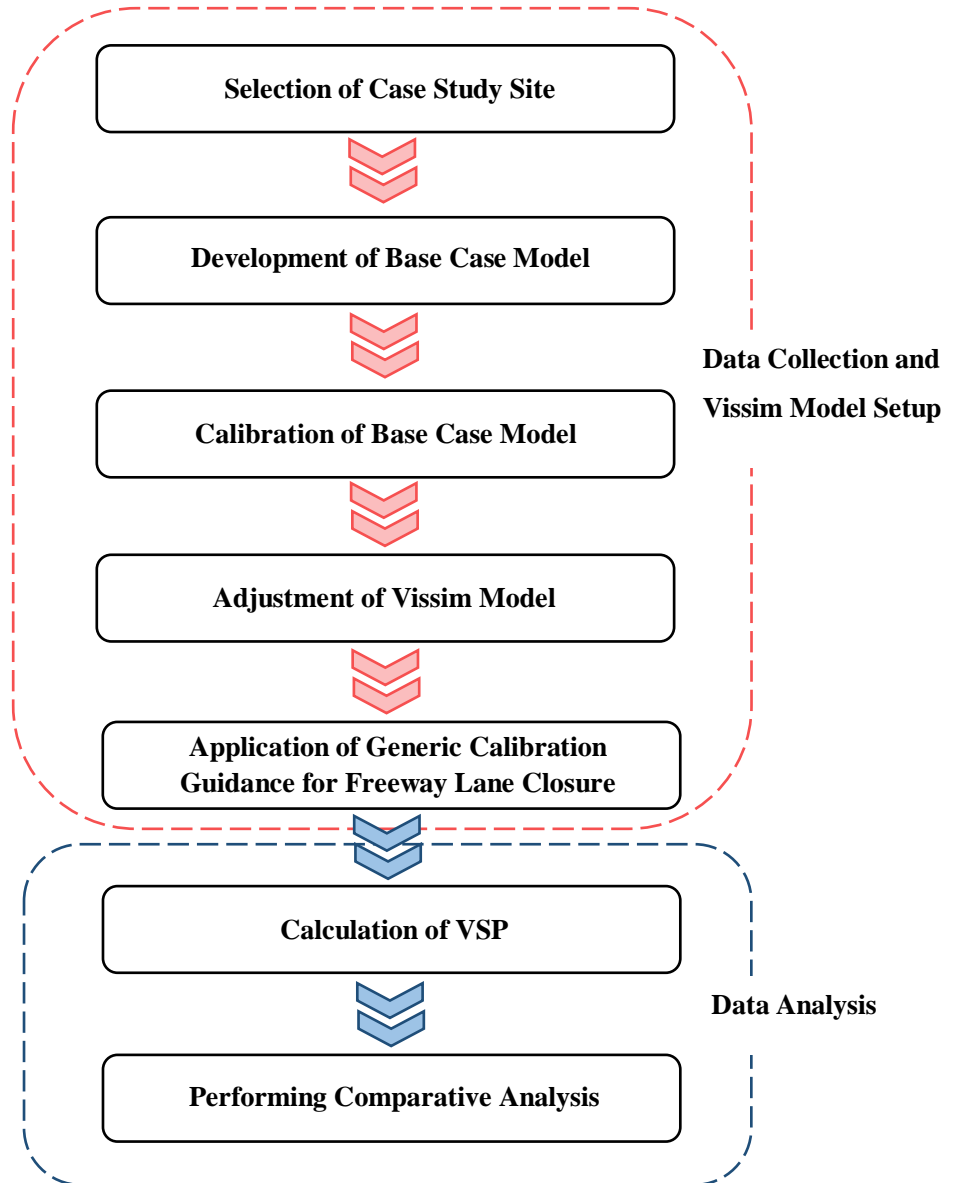
Figure 11. Underlying methodology applied in the research study.

Assessing Effectiveness of Microsimulation Models Using a Case Study

For the purpose of this research, a roadway segment was selected from a previous study conducted by Bou-Saab et al. (*62*) where they examined the impact of work zones on emissions from passenger vehicles at project-level using the SHRP2 naturalistic

driving study data. This will allow comparisons of outputs from Vissim to real-world data in terms of VSP.

The study site in the project included a four-lane divided urban principal arterial segment which is approximately 5 miles long, stretching between Rice and Union road in the Northwest (NW) direction of the New York State Route 400 (NY 400). NY 400, also known as Aurora Expressway, is located within Erie County, NY and can only be accessed through ramps. It connects to Interstate 90 (I-90) in the NW end and terminates at NY 16 in Aurora with a total length of 17 miles. An interchange connecting Highway 20 to NY 400 is present between Rice and Union road. The speed limit on the mainline is 65 mph while the speed is reduced to 25 mph on the ramps. In the SHRP2 study, this particular location in NY had at least one unique work zone with more than 15 traces. A trace is defined as one driver trip through one work zone.

Most recent traffic data for the mainline and ramps were acquired from New York State Department of Transportation (NYSDOT) databases. The data consisted of hourly vehicle counts and speed count averages for the year 2015. However, only short counts were available for the segment of interest, i.e. inventory counts were collected once every three years from portable sensors. Alternatively, continuous traffic counts from a permanent station along a similar expressway segment in Erie County were aggregated to determine the proportion of traffic for each hour of a typical weekday and weekend.

The following criteria were compiled with reference to the lane closure on NY 400 while developing the microsimulation model in Vissim:

- For traffic moving in the NW direction towards I-90 and city of Buffalo, almost 1.5 miles of the roadway section between the interchange and Union road required rehabilitation work on the left lane to restore the condition of the pavement. Expectedly, capacity was reduced due to the 2-to-1 work zone configuration with the closure of the left lane.

- Construction activity occurred in the summer during the month of July. Therefore, it was necessary to adjust the AADT by applying the seasonal factor.

- Traffic was not detoured as vehicles were still capable to access and exit the system through the ramps.

The aerial image in Figure 12 shows the location of the expressway segment including the cloverleaf interchange with ramps connecting to and from the mainline. The markings indicate the extent of the different principal components of a work zone which include:

- Upstream – section of the Aurora expressway before drivers enter the work zone influence area.

- Advanced warning area – consists of traffic control signs warning drivers about an upcoming road closure. In compliance with the Manual on Uniform Traffic Control Devices (MUTCD) (*63)*, the advanced warning area should be 1 mile in length. In other words, the first traffic control sign observed by a driver is 1 mile prior to the start of the lane closure.

- Activity area – as illustrated in Figure 13, lane closure was determined to begin directly before the first exit ramp on the interchange. Rehabilitation work will

take place on the left lane for 1.5 miles of the roadway segment. The desired

speed limit within the vicinity of the activity area is reduced to 45 mph.

- Downstream – where drivers exit the work zone and capacity is restored.

The assumptions/criteria for the advanced warning area and activity area were verified

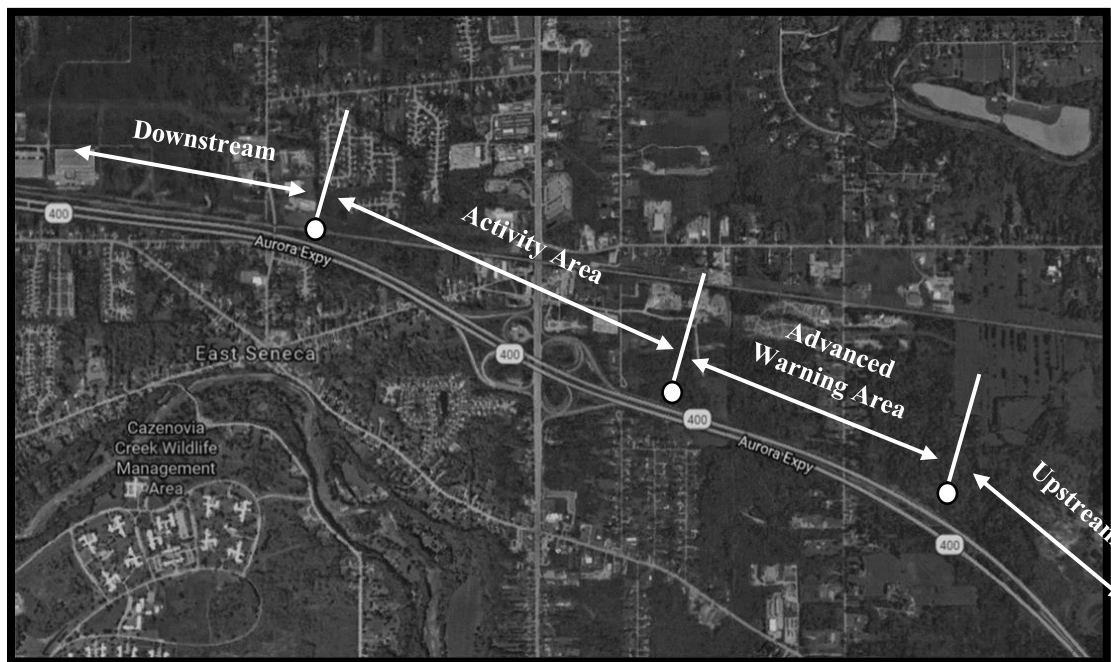from the actual work zone location in the SHRP2 study.

Figure 12. Location of the case study site on Aurora Expressway between Rice and Union road in the NW direction (source: Google Maps).

Figure 13. Left lane closure which started directly before the first exit ramp (source: Google Maps).

Links representing the upstream and downstream in the microsimulation model were

considered to be approximately 0.5 miles in length. Failure to meet the distance

requirement might not capture the underlying complete vehicle operation within these

particular principal components sections of the network. In addition, the paired links

described in Table 8 were assumed in order to generate the hourly origin-destination (O-

D) matrices used as inputs in Vissim.

Table 8. Description of Paired Links Used to Create Origin-Destination Matrices in Vissim

Paired Links	Traffic Flow Assumption/Description
L1 – R1	Vehicles traveling on the mainline segment and exiting through the first exit ramp
L1 – R3	Vehicles traveling on the mainline segment and exiting through the second exit ramp
R2 – L2	Vehicles connecting to the mainline from the first entrance ramp
R4 – L2	Vehicle connecting to the mainline from the second entrance ramp
L1 – L2	Vehicles traveling on the mainline from the beginning until the end of the roadway segment
R2 – R3	None of the vehicles that entered the expressway network from R2 exited through R3

Composition of the different vehicle types in the traffic stream is presented in Table 9. The proportion of vehicles by source type were specifically based on the 2015 traffic data for the road segment on Aurora expressway.

Table 9. Composition of Vehicles by Source Type (Source: 2015 NYSDOT Traffic Data Report)

Vehicle Type	Proportion (%)
Passenger cars	75
Pickup trucks, vans and motor homes	17
Buses	1
Heavy-duty trucks	7

The intent of the study was to evaluate the accuracy of Vissim to generate vehicle trajectories similar to field observations. Different roadway construction scenarios for 2-to-1 lane closure configuration were simulated in Vissim and analyzed to determine how well the microscopic model replicated real-world vehicle operations at the case study location. These scenarios were first applied to the calibrated base model without altering the default car-following and lane changing driver behavior characteristics. A generic guidance proposed by Yeom et al. (*61*) for calibrating work zone capacity on freeways using the car-following and lane changing parameters was also assessed. If the outcomes were identical to field observations from the SHRP2 research project, then practitioners can reliably apply either the default or the calibration guidance to accurately estimate emissions of various traffic transportation strategies for inclusion in CBA. The next generation of models used to estimate emissions in the U.S. require instantaneous speed and acceleration as inputs which can be generated from Vissim. As part of this research effort, the impact of closing the left lane for 1.5 miles on Aurora expressway was assessed in the following construction scenarios:

- Lane closure during AM and PM peak-hour: this scenario is analogous to traditional construction where lane closure typically occurs during the weekday between 7 AM and 5 PM.

- Lane closure during nighttime off-peak hours: it is assumed that rehabilitation work will take place during the weekday at night between 8 PM and 5 AM. Nighttime road work is common in regions with high traffic volumes which makes it difficult to close lanes during the day. This is mainly because disruptions can severely reduce capacity and increase risk for drivers and workers (*64*).

Microsimulation models should ideally run for the entire 24-hour time period. However, this might be challenging since generating and analyzing data at one second intervals is time-consuming and resource intensive. Alternatively, it is advised to focus on certain hours of the day, such as AM and PM peak-hours, since traffic demand is highest during these time periods. According to traffic counts, AM peak-hour for the road segment on Aurora expressway was between 7 and 8 AM. The maximum traffic volume during the PM period was recorded between 5 and 6 PM.

The initial expressway model, explicitly the base case scenario with no interruptions due lane closure, was calibrated using volume and desired speed distribution. Moreover, all models were experimented with 10 random seed numbers. A comparison between the simulated outcomes and actual input volumes suggested that the model was well-calibrated since the difference was less than 2 percent for all random seeds. An initialization period of 15 minutes was also added to the simulation period to ensure that equilibrium was achieved.

Table 10 presents the generic guidance to calibrate the capacity for a 2-to-1 work

zone configuration in Vissim. Only cc1 and cc2 parameters from the Wiedemann 99 car-

following model had to be adjusted depending on the work zone lane configuration. The

other parameters were recommended at their default values. Additionally, all factors in

the lane changing model were fine-tuned. These modifications correlate to the more

cautious driving behavior in a work zone.

Table 10. Generic Guidance for Vissim Capacity Calibration (Source: Yeom et al. 2016)

Parameter	Vissim Default	Recommended Value
Car-Following Model		
cc0 (ft.)	4.92	4.92
cc1 (s)	0.90	$-0.0023 \times$ avg. QDR + 5.3416
cc2 (ft.)	13.12	23.62
cc3 (s)	-8.00	-8.00
cc4 (ft./s)	-0.35	-0.35
cc5 (ft./s)	0.35	0.35
cc6	11.44	11.44
cc7 (ft./s^2)	0.82	0.82
cc8 (ft./s^2)	11.48	11.48
cc9 (ft./s^2)	4.92	4.92
Lane Change Model		
Lane change distance (ft.)	656.20	3,281.00
Necessary lane change, 1 ft./s^2 per distance (ft.)	200.00	100.00
Maximum deceleration for cooperative lane braking (ft./s^2)	-9.84	-20.00

According to Table 10, the value of cc1 parameter can be adjusted using the regression

model developed by the researchers. The model is a function of the average queue

discharge flow rate (avg. QDR) which can be calculated using Equation 1:

$$average\ QDR = 2{,}093 - 154\ (f_{LCSI}) - 194\ (f_{barrier}) - 179\ (f_{area}) + 9\ (f_{lateral\_12}) - 59\ (f_{day\_night}) \quad (1)$$

Where,

$average\ QDR$:	measured in passenger cars per hour per lane (pcphpl)
f_{LCSI}:	1 / (open ratio × number of open lanes)
$f_{barrier}$:	0 for concrete, 1 for soft (cone or polyethylene drums)
f_{area}:	0 for urban and 1 for rural
$f_{lateral\_12}$:	lateral clearance – 12 ft. (minimum value is -11.9 ft. and maximum value is 0 ft.)
f_{day_night}:	0 for day and 1 for night
Open ratio:	number of open lanes to total number of lanes

Taking into consideration that the principal arterial roadway segment is in an urban area and soft drums are used to close the left lane with no lateral clearance, the avg. QDR for the AM and PM peak-hour traffic is equivalent to 1,484 pcphpl. The minimum value for $f_{lateral\_12}$, i.e. -11.9 ft., is applied in the equation since it is assumed that the lateral distance from the edge of travel lane adjacent to the work zone to the barrier is zero. Expectedly, the value of avg. QDR is reduced to 1,425 pcphpl for the nighttime construction scenario. Table 11 provides the cc1 estimates for the different lane closure scenarios.

Table 11. Estimated cc1 Parameters for the Different Road Rehabilitation Scenarios

Construction Scenario	Estimated Recommended cc1 Parameter (s)
AM peak-hour lane closure	1.90
PM peak-hour lane closure	1.90
Nighttime off-peak lane closure	2.04

Adhering to the calibration guidance, the driving behavior parameters were applied to both the advanced warning and activity area links. Adjustment for the lane change distance was only implemented on the connector between the advanced warning area and the lane drop. The average and standard deviation of the desired speed were changed throughout the work zone to 47.9 and 3.1 mph, respectively. Modeling the reduced speed area will guarantee that vehicles decelerate prior to the lane drop point.

The base case and lane closure Vissim models were simulated for the morning

and evening peak as well as the nighttime off-peak hours. Following the extraction of

output files, databases were queried to exclude pickup trucks, buses and heavy vehicles

since field data from SHRP2 were only available for passenger cars. Differences between

vehicle operations on the highway and ramp segments exist, therefore only vehicle

trajectories on the mainline were considered for analysis. Furthermore, the databases for

the lane closure scenarios were separated according to their principal area component.

Analysis

Results from field observations and Vissim were compared using VSP. Vehicle emissions

are directly correlated to the instantaneous engine load demand and VSP has been used as

a surrogate variable for power demand or engine load (*65*). Predominantly, speed,

acceleration, road grade and air conditioning use have significant impact on engine load.

The second-by-second vehicle activity data from Vissim were used as inputs for the VSP

equation:

$$VSP = \left(\frac{A}{M}\right)v + \left(\frac{B}{M}\right)v^2 + \left(\frac{C}{M}\right)v^3 + (a + g\sin\theta)v \tag{2}$$

Where,

A is the road load coefficient for rolling resistance (kW-s/m) = 0.1564

B is the road load coefficient for rotating resistance (kW-s^2/m^2) = 0.0020

C is the road coefficient for drag resistance (kW-s^3/m^3) = 0.00049

M is the fixed mass facto for vehicle source type (metric tons) = 1.4788

g is acceleration due to gravity (m/s^2)

v is vehicle speed (m/s)

a is vehicle acceleration (m/s^2)

sin θ is fractional road grade

The coefficients for *A*, *B*, *C* and *M* were obtained from the MOVES 2014 highway vehicle population and activity data guide. Only passenger cars were assumed in the analysis. In addition, road gradient was assumed to be flat (i.e. $\theta = 0$). These assumptions will ensure better comparisons in emissions by eliminating differences between vehicle types and roadway terrain.

VSP is binned in such a way that three main vehicle operations are represented: deceleration (VSP<0), idling (0≤VSP<1) and cruising/acceleration (VSP>1). Higher emission rates and fuel consumption (per second) are associated with higher VSP bins. The benefit of assessing vehicle trajectories using VSP distribution, is that it captures any erroneous conclusions which might result when aggregating total emissions. Errors from instantaneous results might be eliminated which produces a low overall error (*59*).

Results and Discussion

The results in Figure 14 demonstrate the fraction of time vehicles spent in each VSP bin comparing the advanced warning and activity area components of the work zone from Vissim and SHRP2, respectively. While Figure 15 explains the VSP results by cumulative percent. The analysis targeted the advanced warning and activity components of the work zone since the majority of changes in vehicle operations were expected to occur within these sections of the expressway network. This is also in view of the fact that alterations to driving behavior parameters in Vissim were implemented on these particular principal areas.

Queuing of vehicles before entering the vicinity of the lane closure links was observed from simulation runs, accordingly results from Vissim can be compared to the highly congested VSP distributions from the SHRP2 field observations. As evident from

the SHRP2 NDS results in Figure 14, there is a smooth transition in vehicle operations from higher to lower VSP bins as drivers enter the work zone with the exception of highly congested cases. This is because it was determined from the SHRP2 forward roadway video-logs that as congestion level increased, queues started to form upstream of the lane closure. However, the queues dissipated after vehicles traveled for 0.3 miles inside the activity area. When weighed against the AM and PM peak-hour Vissim outputs, there are similarities in the amount of time vehicles spent idling in the advanced warning area. This is not the case for the activity area, as simulated activity results in Figures 14 and 15 showed that vehicles overestimated idling. Moreover, drivers tended to decelerate/accelerate more frequently. Traffic flow during nighttime was lower than AM and PM peak-hours, therefore activity results from microsimulation were compared to the non-congested and moderately congested distributions from field trajectories. Sharper transitions in VSP bins were recorded as vehicles reduced their speeds to enter the work zone.

The findings were consistent with previous research (*44, 59 and 60*), as the simulated vehicles in Vissim experienced more aggressive accelerations/decelerations, especially at lower speeds where car-following model is the governing factor. Both the default and generic guidance lane closure Vissim scenarios have similarities in the shape of the VSP distributions. This indicates that the default driver behavior parameters must be calibrated and further investigation is required for the generic calibration guidance in order or other optimization techniques should be testes to produce more realistic VSP distributions since both cc1 and cc2 parameters in the car-following model are critical indicators.
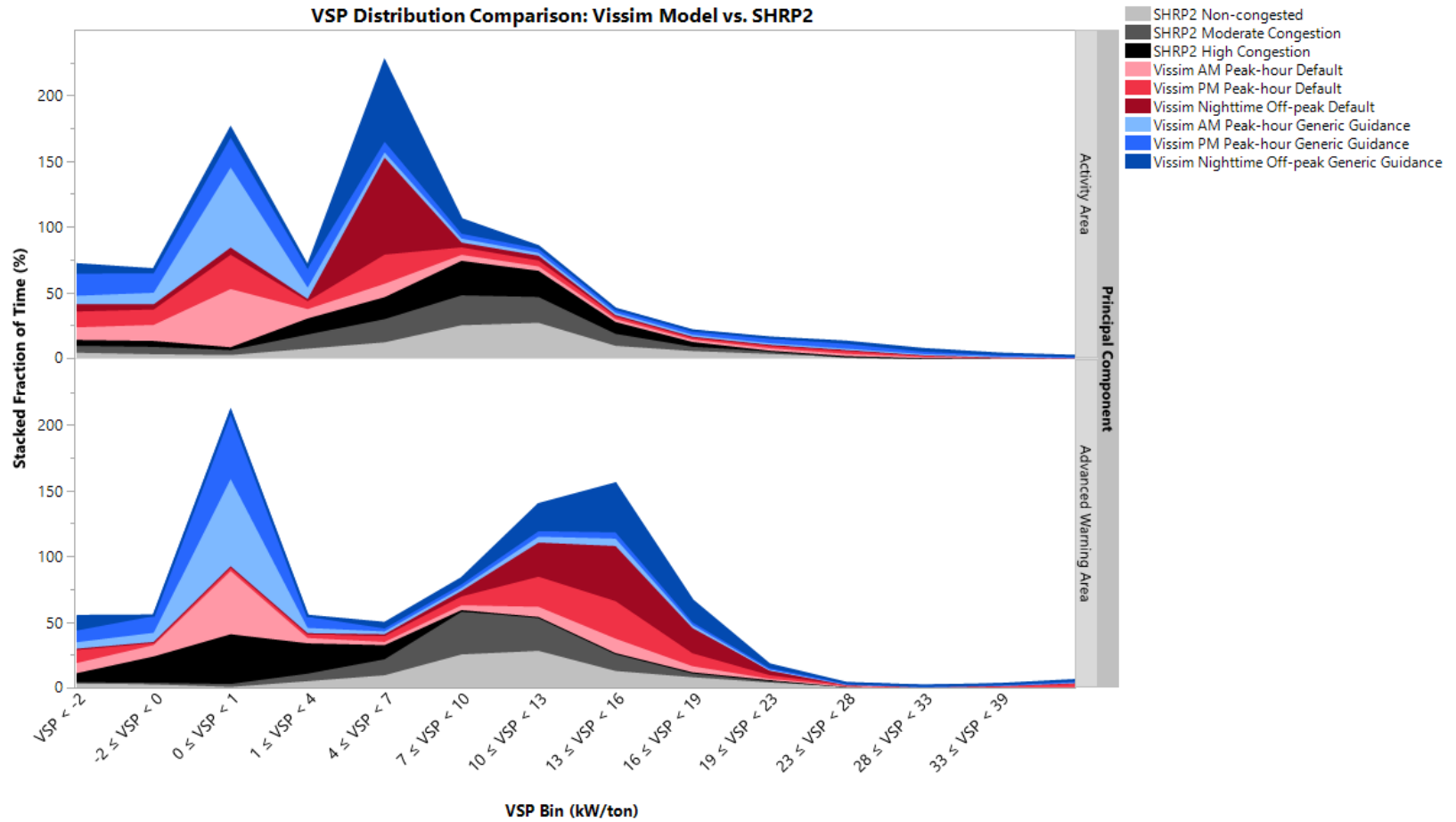
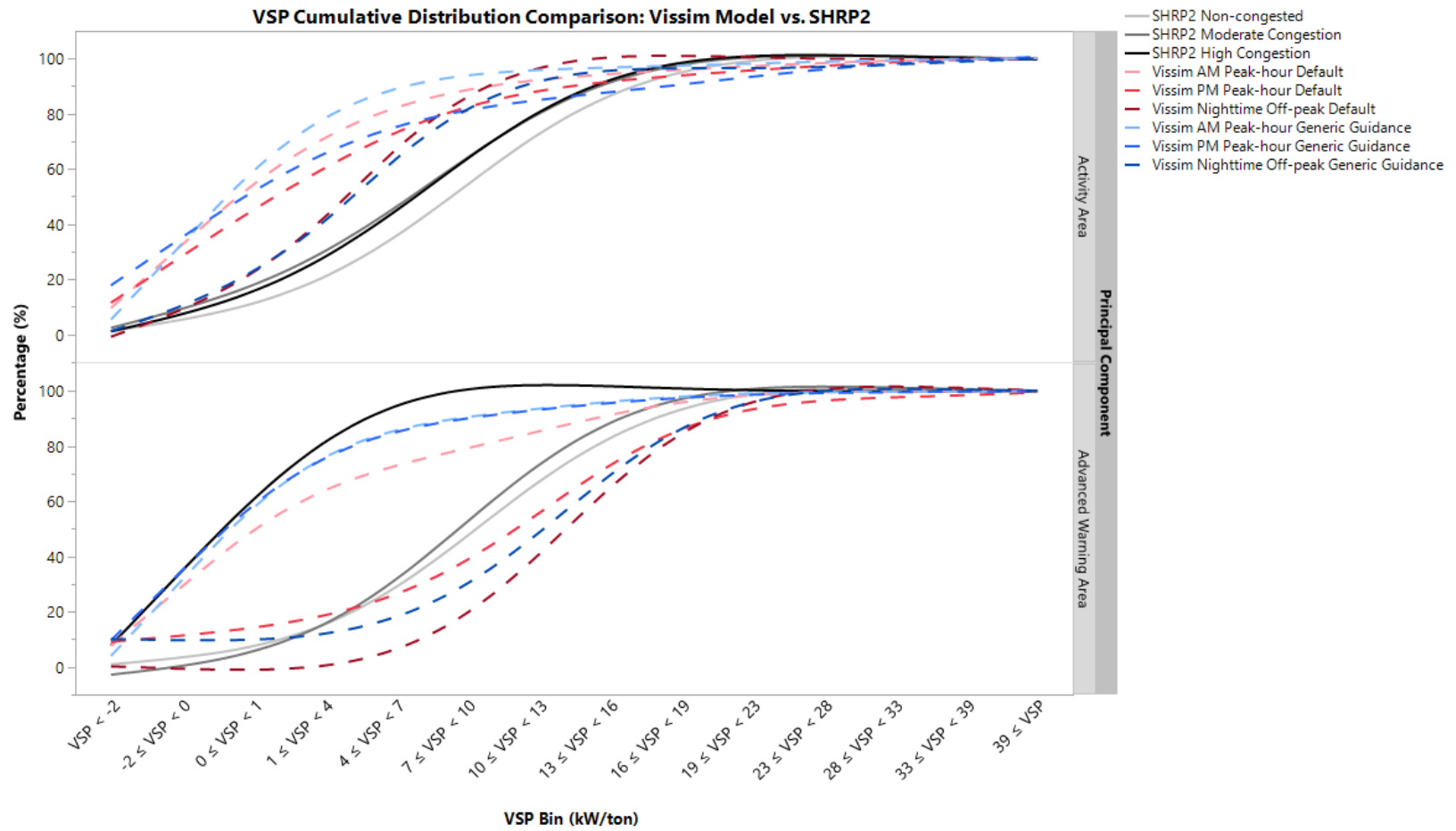**Figure 14. VSP bin distributions comparing Vissim and SHRP2 results.**

Figure 15. VSP cumulative distributions comparing Vissim anSHRP2 results.

To visually illustrate the consistency of VSP and acceleration distribution between

Vissim and SHRP2 observations, 8 speed bins across various speed levels (0-10, 10-20,

20-30, 30-40, 40-50, 50-60, 60-70, and 70+ mph) were selected.

VSP Distribution

The resulting VSP distributions by different speed bins for advanced warning area

in Figure 16 and activity area in Figure 17 demonstrate that Vissim provides less

consistent VSP behavior when compared to the field observations from SHRP2. The

discrepancy in VSP behavior is more apparent within the lane closure (activity area)

portion of the work zone for all speed levels. For both components of the work zone and

low speed levels (speed < 40 mph), the simulated vehicles in Vissim overestimate

distribution in lower VSP region (VSP < -2) which represent the deceleration operating

mode. There is also less consistent VSP behavior in higher speed bins (speed > 50 mph)

since driver behavior is usually widely dissimilar in free driving. Therefore, it becomes

challenging for the Wiedemann car-following model to capture the realistic free driving

behavior overcome (*59*). However, this can be overridden in the case when actual free-
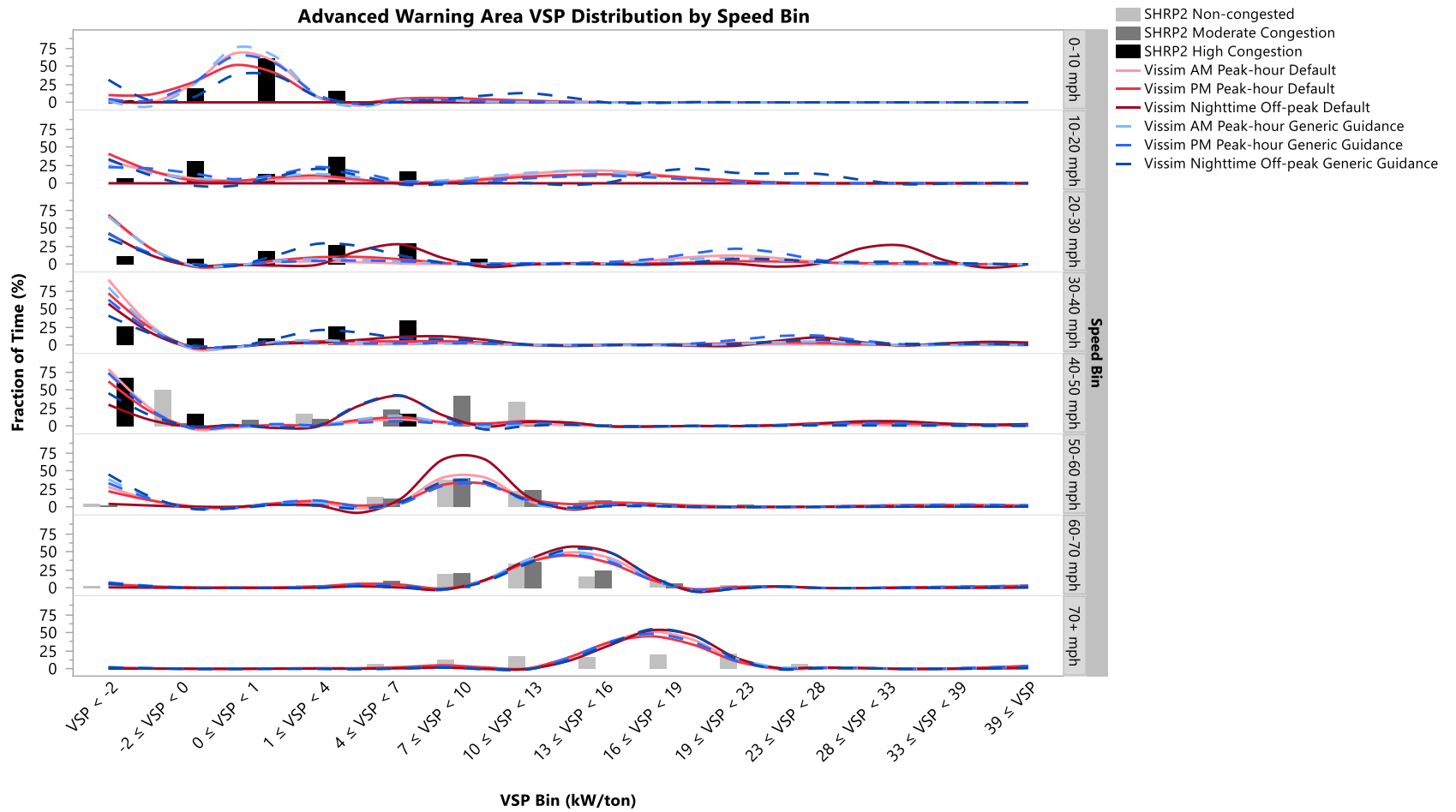
flow speed is used as input for each scenario.

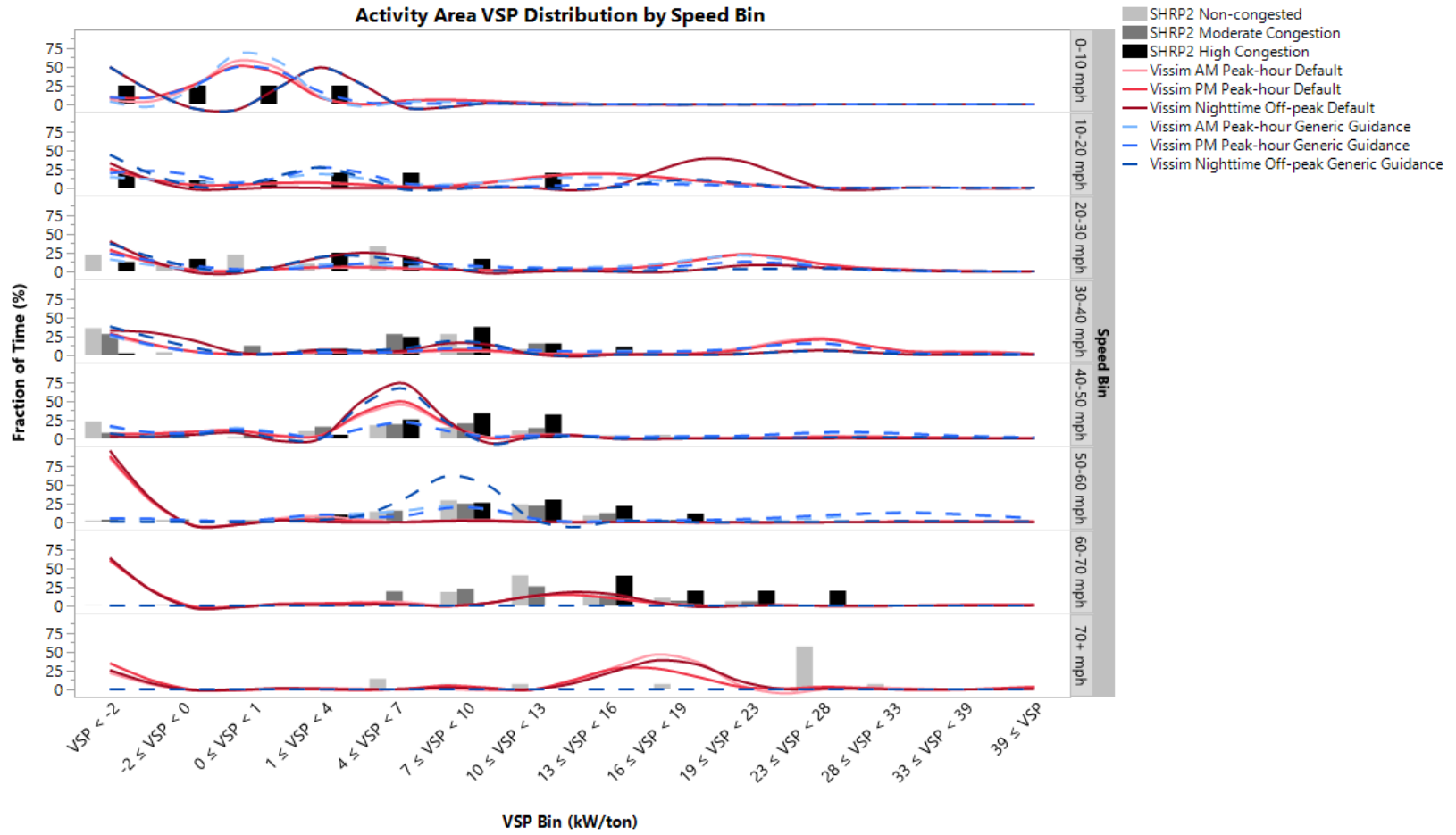Figure 16. Advanced warning area VSP distribution by different speed bins.

Figure 17. Activity area VSP distribution by different speed bins.

Acceleration Behavior

Wang et al. (*59*) comprehensively investigated the acceleration behavior of vehicles at varying speed levels to ascertain the primary source of error in VSP distribution which might be prompted by the Wiedemann car-following model in Vissim. Acceleration distribution is examined because it is known to be the most sensitive parameter to vehicle power. Figures 18 and 19 provide a visual comparative representation between Vissim and SHRP2 for the advanced warning and activity components of the work zone, respectively. In both cases, Vissim generates contradictive acceleration behavior across all speed levels. As shown in Figure 18, Vissim produces highly inconsistent acceleration behavior as the distributions differ for the entire speed range in the advanced warning area. There is also an indication that Vissim overestimates distribution in lower and higher acceleration bins for the low and moderate speed levels. This can be attributed to the high maximum deceleration rate for cooperative lane braking of -20.00 ft./s^2. However, the Wiedemann car-following model produces a better fit at moderate speed levels within the activity area. As a result, the incompetency of Vissim to provide realistic VSP behavior can be explicitly explained by the inconsistencies in acceleration distribution.

Most recognized car-following models, such as Wiedemann, lack the ability to produce realistic acceleration since they inflict impractical vehicle dynamics constraints on the acceleration behavior (*59*). On the other hand, acceleration model is not the only element which has an impact on the acceleration behavior of vehicles. The regime structure of the Wiedemann model is another primary source of error. Previous research (*44, 59 and 60*) showed that there are sharp transitions in acceleration between regimes.
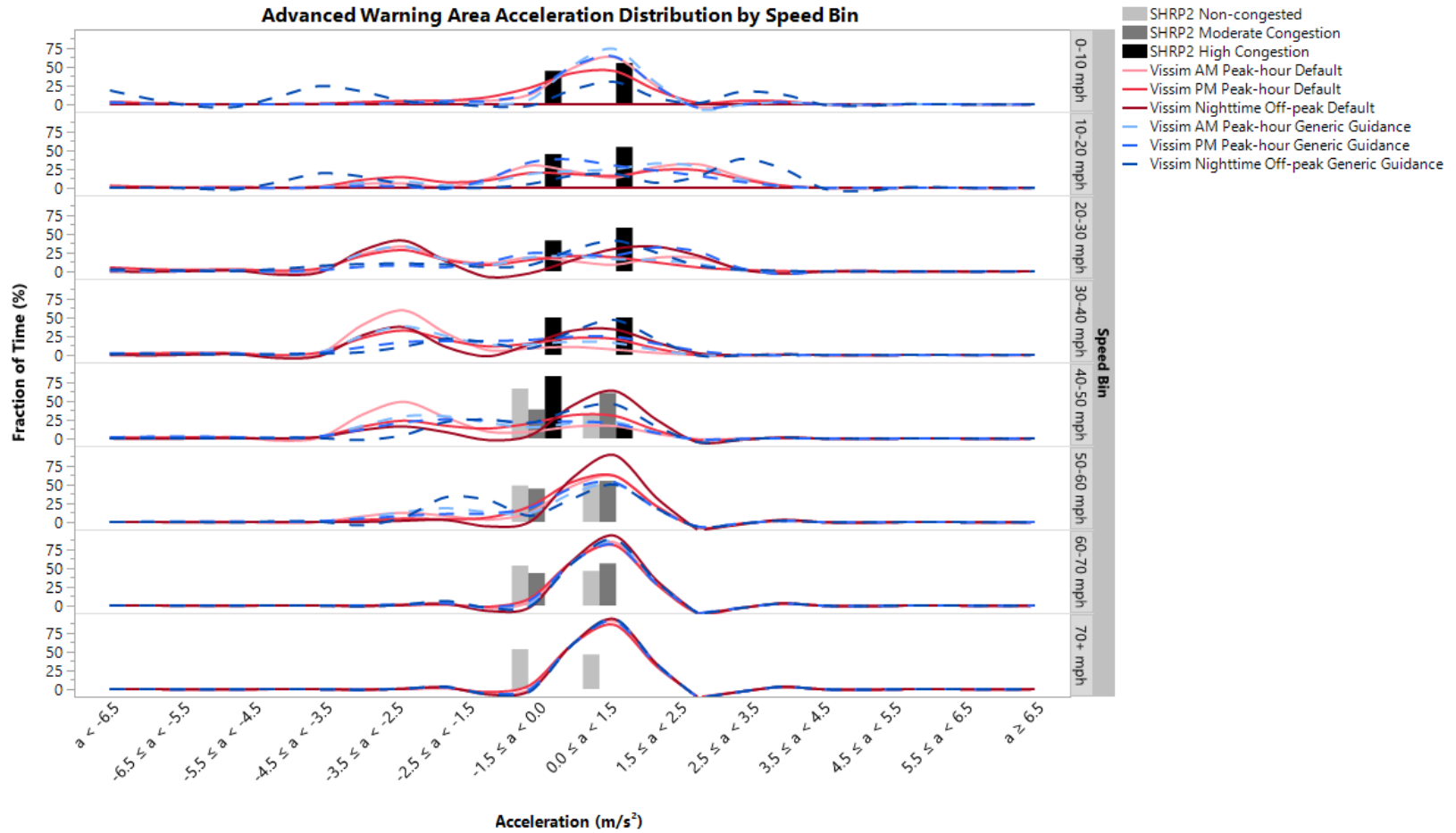
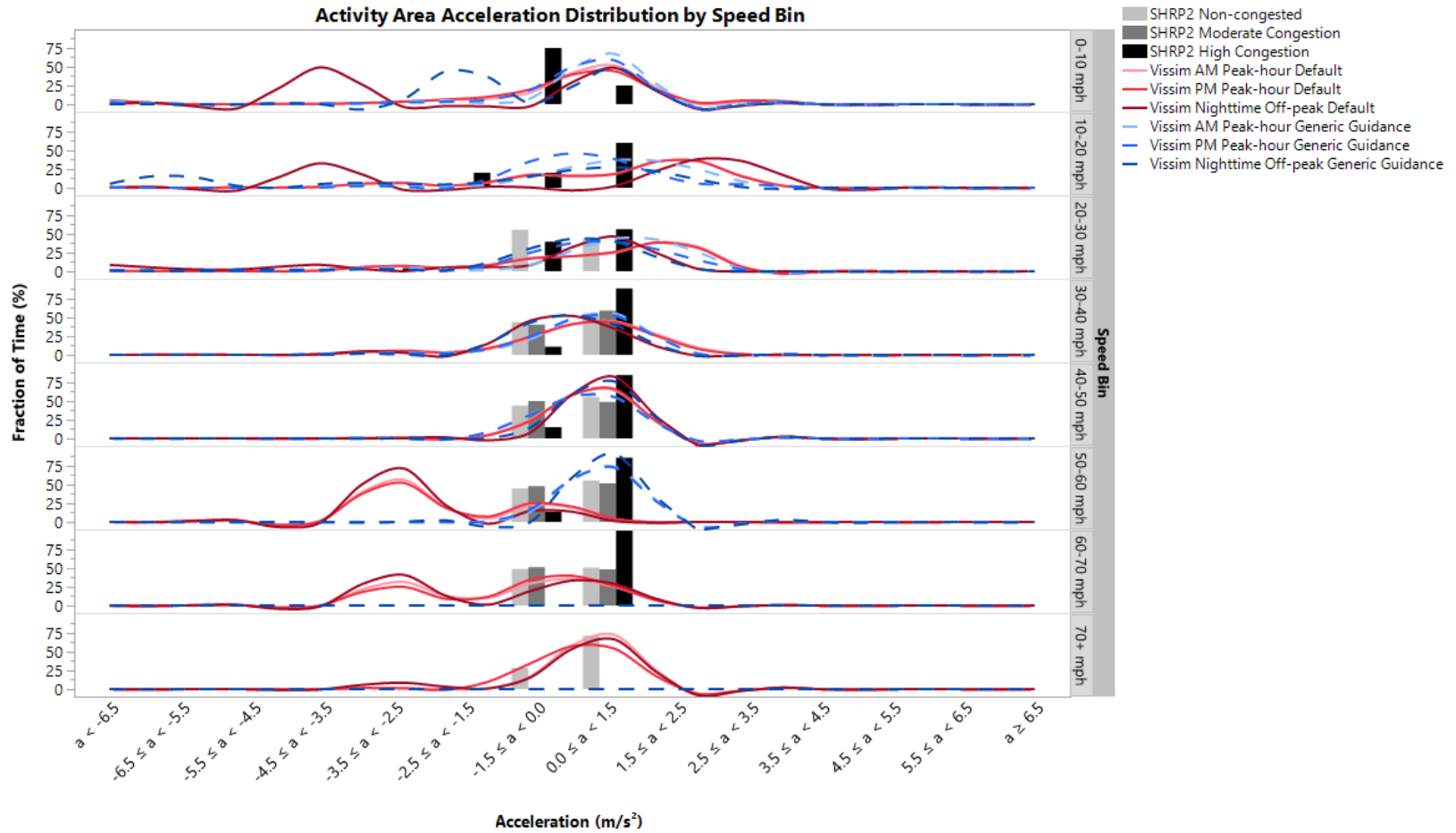**Figure 18. Advanced warning area acceleration distribution by different speed bins.**

Figure 19. Activity area acceleration distribution by different speed bins.

Conclusion

Chapter 3 presented a case study to assess the ability of Vissim to replicate real-world conditions. The trajectories can then be used to model emissions. Hence, it is important for traffic microsimulation models to accurately represent field observations in order to have better emissions estimates. The conclusions for the tasks that were accomplished in this research study are summarized as follow:

- Many researchers depend on microscopic simulation to stochastically model various traffic incident scenarios. They are used as an alternative to field observations. However, previous studies showed that it is necessary to calibrate the car-following and lane changing parameters in order for the microsimulation model to represent field observations with high precision.

- A specific location in Buffalo, NY was used as a case study for the development of the Vissim microsimulation model. It was one of the work zone locations in the SHRP2 naturalistic driving study.

- Three different lane closure scenarios were simulated: AM-peak, PM-peak and nighttime off-peak.

- It was not possible to calibrate the driver behavior parameters in Vissim from the SHRP2 forward roadway video logs. Therefore, a generic calibration guidance was evaluated.

- Results from the work zone scenarios which were merely based on the initial calibrated base models without changing the default driver behavior characteristics indicated that it was necessary to adjust the car-following and lane changing parameters.

- When the generic calibration guidance was applied, findings also showed high
  variability in VSP and acceleration distributions at varying speed levels.

- Moreover, SHRP2 results were based on limited number of traces and congested
  traces might not have occurred during peak hours.

- Transportation agencies are still required to calibrate for local conditions.

References

1. Work Zone Management Program. *Using Modeling and Simulation Tools for Work Zone Analysis*. Office of Operations, FHWA. https://ops.fhwa.dot.gov/wz/traffic_analysis/wza_leaflet/wza_leaflet.htm. Accessed January 27, 2019.

2. Mashayekh, Y., P. Jaramillo, M. Chester, C. T. Hendrickson and C. L. Weber. Costs of Automobile Air Emissions in U.S. Metropolitan Areas. *Transportation Research Record: Journal of the Transportation Research Board*, 2011. 2233: 120 – 127.

3. Couture, L-E., S. Saxe and E. J. Miller. Cost-Benefit Analysis of Transportation Investment: A Literature Review. University of Toronto Research Institute. https://uttri.utoronto.ca/. Accessed February 5, 2019.

4. *Cost/Benefit Analysis of NJDOT Route 18/Hoes Lane Improvement Project for TIGER II Grant Application*. New Jersey Department of Transportation. https://www.state.nj.us/transportation/works/studies/rt18_i287connect/pdf/cb_analysis.pdf. Accessed February 2, 2019.

5. Meunier, D. and E. Quinet. Valuing Greenhouse Gases Emissions and Uncertainty in Transport Cost Benefit Analysis. *Transportation research Procedia*, 2015. 8: 80 – 88.

6. Dia, H. and W. Gondwe. Evaluation of Incident Impacts on Integrated Motorway and Arterial Networks Using Traffic Simulation. Presented at the 31st Australasian Transport Research Forum, Gold Coast, Australia, 2008.

7. Jie, L., H. Van Zuylen, Y. Chen, F. Viti and I. Wilmink. Calibration of a Microscopic Simulation Model for Emission Calculation. *Transportation Research Part C: Emerging Technologies*, 2013. 31: 172 – 184.

8. Mallela, J. and S. Sadasivam. *Work Zone Road User Costs – Concepts and Applications*. Publication FHWA-HOP-12-005. FHWA, U.S. Department of Transportation, 2011.

9. Lemp, J. and K. Kockelman. Quantifying the External Costs of Vehicle Use: Evidence from America's Top-Selling Light Duty Models. *Transportation Research Part D: Transport and Environment*, 2008. 13: 491 – 504.

10. Planning and Programming. *Benefit-Cost Analysis for Transportation Projects*. Minnesota Department of Transportation. https://www.dot.state.mn.us/planning/program/benefitcost.html. Accessed January 28, 2019.

11. *Economic Analysis Primer*. Office of Asset Management, FHWA. https://www.fhwa.dot.gov/publications/focus/03nov/03.cfm. Accessed February 10, 2019.

12. Williges, C. and M. Mahdavi. Transportation Benefit-Cost Analysis: It's All about Inputs!. Presented at the benefit-Cost Analysis Conference, Seattle, Washington, 2007.

13. Litman, T.A. and E. Doherty. *Transportation Cost and Benefit Analysis: Techniques, Estimated and Implications*. Victoria Transport Policy Institute. http://www.vtpi.org/tca/. Accessed February 2, 2019.

14. Jones, H., T. Domingos, F. Moura and J. Sussman. Transport Infrastructure Evaluation Using Cost-Benefit Analysis: Improvements to Valuing the Asset through Residual Value – A Case Study.

15. Iacono, M. J. and D. M. Levinson. Methods for Estimating the Economic Impacts of Transportation Improvements: An Interpretive Review. Edward Elgar Publishers. University of Minnesota Digital Conservancy. http://hdl.handle.net/11299/180056. Accessed January 28, 2019.

16. Beukers, E., L. Bertolini, and M. Te Brömmelstroet. Why Cost Benefit Analysis is Perceived as a Problematic Tool for Assessment of Transport Plans: A Process Perspective. *Transportation Research Part A: Policy and Practice*, 2012. 46: 68 – 78.

17. Quinet, E. A Meta-Analysis of Western European External Costs Estimates. *Transportation Research Part D: Transport and Environment*, 2004. 9: 465 – 476.

18. Geurs, K. T., W. Boon and B. Van Wee. Social Impacts of Transport: Literature Review and the State of the Practice of Transport Appraisal in the Netherlands and the United Kingdom. *Transport Reviews*, 2009. 29: 69 – 90.

19. Gao, Y. *Calibration and Comparison of the VISSIM and INTEGRATION Microscopic Traffic Simulation Models*. Master Thesis, Virginia Polytechnic Institute and State University. https://vtechworks.lib.vt.edu/handle/10919/35005. Accessed January 15, 2019.

20. Dia, H. and W. Gondwe. Evaluation of Incident Impacts on Integrated Motorway and Arterial Networks Using Traffic Simulation. Presented at the 31st Australasian Transport Research Forum, Gold Coast, Australia, 2008.

21. Swidan, H. *Integrating AIMSUN Micro Simulation Model with Portable Emissions Measurement System (PEMS): Calibration and Validation Case Study*. Master Thesis, North Carolina State University. https://repository.lib.ncsu.edu/bitstream/handle/1840.16/7275/etd.pdf?sequence=2 . Accessed January 15, 2019.

22. Hidas, P. Modelling Individual Behavior in Microsimulation Models. Presented at the 28th Australasian Transport Research Forum, Sydney, Australia, 2005.

23. Hallmark, S. S. Chrysler and N. Oneyear. *Validation of Traffic Simulation Model Output for Work Zone and Mobile Source Emissions Modeling and Integration with Human-in-the-Loop Driving Simulators*. Mid-America Transportation Center Publication WBS: 25-1121-0003-138. Accessed February 2, 2019.

24. Khanta, P. R. *Evaluation of Traffic Simulation Models for Work Zones in the New England Area*. Master Thesis, University of Massachusetts Amherst. https://scholarworks.umass.edu/theses/184/. Accessed January 10, 2019.

25. Chiappone, I. S. *Traffic Fundamentals for A22 Brenner Freeway by Microsimulation Models*. Doctor of Philosophy Dissertation. https://iris.unipa.it/retrieve/handle/10447/160235/255699/. Accessed January 15, 2019.

26. Madi, M. Y. Investigating and Calibrating the Dynamics of Vehicles in Traffic Micro-simulations Models. *Transportation Research Procedia*, 2016. 14: 1782 – 1791.

27. Jackson, E., and L. Aultman-Hall. Analysis of Real-World Lead Vehicle Operation for Integration of Modal Emissions and Traffic Simulation. Presented at 89th Annual Meeting of the Transportation Research Board, Washington, D.C., 2010.

28. Dowling, R. A. Skabardonis, V. Alexiadis. *Traffic Analysis Toolbox Volume III: Guidelines for Applying Traffic Microsimulation Software*. Publication FHWA-HRT-04-040. FHWA, U.S. Department of Transportation, 2004.

29. Espejel-Garcia, D., J. A. Saniger-Alba, G. Wenglas-Lara, V. V. Espejel-Garcia and A. Villalobos-Aragon. A Comparison among Manual and Automatic Calibration Methods in VISSIM in an Expressway (Chihuahua, Mexico). *Open Journal of Civil Engineering*, 2017. 7: 539 – 552.

30. Lu, X-Y., J. Lee, D. Chen, J. Bared, D. Dailey and S.E. Shladover. Freeway Micro-simulation Calibration: Case Study Using Aimsun and VISSIM with Detailed Field Data. Presented at 93rd Annual Meeting of Transportation Research Board, Washington, D.C., 2014.

31. Dong, J., A. J. Houchin, N. Shafieirad, C. Lu and N. R. Hawkins. *VISSIM Calibration for Urban Freeways*. Center for Transportation Research and Education, Iowa State University. https://lib.dr.iastate.edu/. Accessed January 10, 2019.

32. Zhang, L., G-L. Chang, S. Zhu, C. Xiong, L. Du, M. Mollanejad, N. Hopper and S. Mahapatra. Integrating an Agent-Based Travel Behavior Model with Large-Scale Microscopic Traffic Simulation for Corridor-Level and Subarea Transportation Operations and Planning Applications. *Journal of Urban Planning and Development*, 2013. 139: 94 – 103.

33. Hadiuzzaman, Md. Y. Zhang, T. Z. Qiu, M. Lu and S. AbouRizk. Modeling the Impact of Work-Zone Traffic Flows upon Concrete Construction: A High Level Architecture Based Simulation Framework. *Canadian Journal of Civil Engineering*, 2014. 41: 144 – 153.

34. Park, B. and H. Qi. Microscopic Simulation Model Calibration and Validation for Freeway Work Zone Network – A Case Study of VISSIM. Presented at IEEE Intelligent Transportation Systems Conference, Toronto, Canada, 2006.

35. Zhang, C., S. Liu, J. Ogle, M. Zhang. Micro-simulation of Desired Speed for Temporary Work Zone with a New Calibration Method. *Promet – Traffic and Transportation*, 2016. 28: 49 – 61.

36. Hallmark, S. and N. Oneyear. *Modeling Merging Behavior at Lane Drops*. Institute for Transportation, Iowa State University. https://lib.dr.iastate.edu/. Accessed January 10, 2019.

37. Smadi, A. and J. Baker. *Integrating Planning and Operations Models to Predict Work Zone Traffic*. Advanced Traffic Analysis Center, Upper Great Plains Transportation Institute, North Dakota State University, Fargo, North Dakota, 2008. http://library.nd.gov/. Accessed January 20, 2019.

38. Tympakianaki, A. A. D. Spiliopoulou, A. Kouvelas and M. Papageorgiou. Real-time Merging Traffic Control for Throughput Maximization at Motorway Work Zones. *Procedia - Social and Behavioral Sciences*, 2012. 48: 1545 – 1556.

39. Hourdos, J. and F. Hong. *TH-36 Full Closure Construction: Evaluation of Traffic Operations Alternatives*. Publication MN/RC 2010-04. Minnesota Department of Transportation, 2010.

40. Standridge, C. R., S. Choudhuri, D. Zeitler and S. Khasnabis. *Management and Analysis of Michigan Intelligent Transportation Systems Center Data with Application to the Detroit Area I-75 Corridor, Project 1*. Publication RC-1545. Michigan Department of Transportation, 2010.

41. Lipari, A., C. Caprani and E. O'Brien. Micro-simulation Modelling of Congestion due to Lane Closures. Presented at the Irish Transport Research Network, University of Ulster, Northern Ireland, 2012.

42. Gomes, G. A. May and R. Horowitz. Calibration of VISSIM for a Congested Freeway. Institute of transportation Studies, University of California, Berkeley. https://horowitz.me.berkeley.edu/Publications_files/All_papers_numbered/Gomes_may_horowitz_PATH_report04.pdf. Accessed January 25, 2019.

43. Li, Y., J. C. M. Mori and D. B. Work. *Improving the Effectiveness of Smart Work Zone Technologies*. Publication FHWA-ICT-16-021. Illinois Department of Transportation, 2016.

44. Song, G., L. Yu and L. Xu. Comparative Analysis of Car-Following Models for Emissions Estimation. *Transportation Research Record: Journal of the Transportation Research Board*, 2013. 2341: 12 – 22.

45. Shabihkhani, R. and E. Gonzales. Analytical model for vehicle emissions at signalized intersection: Integrating traffic and microscopic emissions models. Presented at 92nd Annual Meeting of Transportation Research Board, Washington, D.C., 2013.

46. Abou-Senna, H., E. Radwan, K. Westerlund and C. Cooper. Using a Traffic Simulation Model (VISSIM) with an Emissions Model (MOVES) to Predict Emissions from Vehicles on a Limited-Access Highway. *Journal of Air and Waste Management Association*, 2013. 63: 819 – 831.

47. Chamberlin, R., B. Swanson, E. Talbot, J. Dumont and S. Pesci. 2011. Analysis of MOVES and CMEM for Evaluating the Emissions Impact of an Intersection Control Change. Presented at 90th Annual Meeting of Transportation Research Board, Washington, D.C., 2011.

48. Hulsberg, J., 2013. *Emissions Modeling and Implementation into CORISM*. Master Thesis, University of Florida, Gainesville. http://cms.uflib.ufl.edu/etd/Index.aspx. Accessed February 15, 2019.

49. Vincenzo, P., M. Borzacchiellob and B. Ciuffo. On the Assessment of Vehicle Trajectory Data Accuracy and Application to the Next Generation SIMulation (NGSIM) Program Data. *Transportation Research Part C: Emerging Technologies*, 2011. 19: 1243 – 1262.

50. Ahn, K., H. Rakha, A. Trani and M. Van Aerde. Estimating Vehicle Fuel Consumption and Emissions based on Instantaneous Speed and Acceleration Levels. *Journal of Transportation Engineering*, 2002. 128: 182 – 190.

51. Zhai, Z., G. Song and Y. Lu. A Comparative Analysis on Methods of Using Second-By-Second Vehicle Speed Profiles and Operating Mode Distributions for Real-Time Emissions Estimations at the Link Level. Presented at 97th Annual Meeting of Transportation Research Board, Washington, D.C., 2018.

52. Dias, H.L.F., B. V. Bertoncini, M. L. M. de Oliveira, F. S. A. Cavalcante and E. P. Lima, E.P. Analysis of Emission Models Integrated with Traffic Models for Freight Transportation Study in Urban Areas. *International Journal of Environmental Technology and Management*, 2017. 20: 60 – 77.

53. Samaras, C., D. Tsokolisa, S. Toffolob, G. Magrab, L. Ntziachristosa and Z. Samaras. Improving Fuel Consumption and CO_2 Emissions Calculations in Urban Areas by Coupling a Dynamic Micro Traffic Model with an Instantaneous Emissions Model. *Transportation Research Part D: Transport and Environment*, 2018. 65: 772 – 783.

54. Hallmark, S.L. and R. Guensler. Comparison of Speed-Acceleration Profiles from Field Data with NETSIM Output for Modal Air Quality Analysis of Signalized Intersections. *Transportation Research Record: Journal of the Transportation Research Board*, 1999. 1664: 40 – 46.

55. Rakha, H., M. Snare, F. Dion. Vehicle Dynamics Model for Estimating Maximum Light-Duty Vehicle Acceleration Levels. *Transportation Research Record: Journal of the Transportation Research Board*, 2004. 1883: 40 – 49.

56. Zuylen, H., J. Li, Y. Chen, F. Viti and I. Wilmink. Optimizing Traffic Control for Emissions with a Valid Simulation Program – The Calibration of a Simulation Model for Emission Estimation. Presented at 90th Annual Meeting of Transportation Research Board, Washington, D.C., 2011.

57. Hirschmann, K., M. Zallinger, M. Fellendorf and S. Hausberger. 2010. A New Method to Calculate Emissions with Simulated Traffic Conditions. Presented at the 13th IEEE Annual Conference on Intelligent Transportation Systems, 2010.

58. Grote, M., I. Williams, J. Preston and S. Kemp. Including Congestion Effects in Urban Road Traffic CO_2 Emission Modeling: Do Local Government Authorities

have the Right Options?. *Transportation Research Part D: Transport and Environment*, 2016. 65: 95 – 106.

59. Wang, J., H. Rakha and K. Fadhloun. Validation of the Rakha-Pasumarthy-Adjerid Car-Following Model for Vehicle Fuel Consumption and Emission Estimation Applications. *Transportation Research Part D: Transport and Environment*, 2017. 55: 246 – 261.

60. Song, G., L. Yu and Z. Geng. Optimization of Wiedemann and Fritzsche Car-Following Models for Emission Estimation. *Transportation Research Part D: Transport and Environment*, 2015. 34: 318 – 329.

61. Yeom, C., N. M. Rouphail, W. Rasdorf and B. J. Schroeder. Simulation Guidance for Calibration of Freeway Lane Closure Capacity. *Transportation Research Record: Journal of the Transportation Research Board*, 2016. 2553: 82 – 89.

62. Bou-Saab, G., S. Hallmark and O. Smadi. Beyond Safety: Utilizing SHRP2 NDS Data to Model Vehicular Emissions from Passenger Cars at Work Zones Using Vehicle Specific Power and Operating Mode Distribution Approach**.** Presented at 98th Annual Meeting of Transportation Research Board, Washington, D.C., 2019.

63. Part 6: Temporary Traffic Control. In *Manual on Uniform Traffic Control Devices*. FHWA, U.S. Department of Transportation, 2009, pp. 547 – 730.

64. Work Zone Management Program. *Night Work/Off Peak Work*. Office of Operations, FHWA. https://ops.fhwa.dot.gov/wz/construction/night_offpeak_wrk.htm. Accessed February 7, 2019.

65. Frey, H. C., N. M. Rouphail, H. Zhai, T. L. Farias and G. A. Goncalves. Comparing Real-World Fuel Consumption for Diesel- and Hydrogen-Fueled Transit Buses and Implication for Emissions. *Transportation Research Part D Journal*, Vol. 12, 2007, pp. 281 – 291.

CHAPTER 4. GENERAL CONCLUSIONS

The FHWA reported that roadway construction sites cause traffic flow disruptions in a transportation network. Subsequently, this can have an adverse impact on emissions from vehicles. With limited studies related to emissions modeling at work zones, this research paper in Chapter 2 examined the impact of work zones on emissions from passenger vehicles at project-level using SHRP2 NDS data. Emissions from mobile sources are a function of instantaneous changes in vehicle operation and SHRP2 NDS is an eminent source of such data. More than 5.5 million trips and 135 billion seconds of vehicle kinematics were collected from approximately 4,000 drivers in six different states. The emissions models in this study considered work zone principal areas and configuration, as well as varying congestion levels. Results from a case study in Buffalo, NY demonstrated that level of congestion was the main contributing factor for changes in average emissions for criteria pollutants and CO_2. However, aggregating total emissions usually results in imprecise conclusions due to high error margins. Therefore, it is necessary to assess the main inputs, i.e. vehicle trajectories. When the different bivariate speed and accelerations distributions were compared using the energy statistics, results showed that work zone configuration and principal area also had a significant impact on vehicle operations. Findings from this study can be implemented in decision-making policies. Transportation officials and engineers will have the ability to decide on the appropriate lane closure configuration to implement given roadway and traffic characteristics.

The research study in Chapter 3 focused on the precision of estimating the environmental impacts in terms of emissions from mobile sources at work zones using

Vissim. This will provide agencies with an opportunity to determine the efficacy of implementing a particular incident management plan using cost-benefit analysis, one of the common economic evaluation methods in transportation. Professionals can make deliberate decisions during the process of selecting the best project alternative.

Predicting emissions at the project-level requires disaggregate data inputs but the lack of field observations is a challenge encountered by numerous local transportation agencies. Hence, microscopic traffic simulation is recommended to model traffic flow in a network. It is well-established that microsimulation models must be calibrated and validated using local data. Findings showed that it was necessary to calibrate the Vissim model. Consequently, a generic guidance for calibrating capacity at work zones was applied in this project to evaluate the ability of Vissim to replicate field conditions. Three different construction scenarios were implemented, i.e. AM-peak hour, PM-peak hour and nighttime off-peak lane closure. For all the roadway construction scenarios, results showed that the Wiedemann car-following model in Vissim produced highly variable VSP and acceleration distributions relative to the field observations from an earlier SHRP2 publication.

Limitations and Future Research

It should be noted that the research study in Chapter 2 had constraints as some conclusions were drawn from a limited number of data points. For better efficacy, more data points will be required to show any differences in emissions by rural/urban designation, work zone principal area and configuration. This can be accomplished by reducing more traces or fewer categories can be used to create larger data groups.

Furthermore, future research initiatives will include multi-lane divided highways since this study only analyzed work zones located in 4-lane divided principal arterials. Finally, mixed effects regression models can be developed to predict emissions as a function of significant independent variables, such as type of barrier, drivers' demographics, roadway characteristics and etc.

The generic calibration process tested in Chapter 3 was built on a simplistic model which only considered links indicating the advanced warning and activity components of the work zone. Hence, it did not fit the case study presented in this research effort because ramps were included due to the presence of an interchange. Ramps might have impacted the findings due to lane merging. It should also be noted that some of the results from SHRP2 were based on limited number of observations, more specifically for the high congestion traces. Additionally, congestion in the real-world observations, i.e. SHRP2 NDS might have occurred due to reduction in capacity but not necessarily during AM and PM peak-hours. Microsimulation modeling is regarded as an effective tool to assess how different transportation strategies might have an impact on the traffic stream in a network. To this point, in order to overcome the limitations of Vissim, it is still critical to collect site-specific data to calibrate work zone models and optimize the car-following and lane changing characteristics.